Journal of Cerebral Blood Flow & Metabolism (2010) 30, 187–195
 0271-678X/10 $32.00
www.jcbfm.com

Measurement error analysis for the determination of dopamine D_2 receptor occupancy using the agonist radioligand [^{11}C]MNPA

Miho Shidahara[1], Hiroshi Ito[2], Tatsui Otsuka[2], Yoko Ikoma[2,3], Ryosuke Arakawa[2], Fumitoshi Kodaka[2], Chie Seki[1], Harumasa Takano[2], Hidehiko Takahashi[2], Federico E Turkheimer[4], Yuichi Kimura[1], Iwao Kanno[1] and Tetsuya Suhara[2]

[1]*Biophysics Group, Molecular Imaging Center, National Institute of Radiological Sciences, Chiba, Japan;* [2]*Molecular Neuroimaging Group, Molecular Imaging Center, National Institute of Radiological Sciences, Chiba, Japan;* [3]*Department of Investigative Radiology, National Cardiovascular Center Research Institute, Osaka, Japan;* [4]*Department of Clinical Neuroscience, Division of Neuroscience and Mental Health, Imperial College London, London, UK*

The purpose of this study is to investigate errors in quantitative analysis for estimating dopamine D_2 receptor occupancy of antipsychotics with agonist radioligand [^{11}C]MNPA by numerical simulation, with particular attention to the validity of a quantitative approach based on the use of a reference region. Synthetic data were validated using clinical data combined with a bootstrap approach. Time–activity curves (TACs) of [^{11}C]MNPA were simulated, and the reliability of binding potential (BP_{ND}) and occupancy estimated by nonlinear least square (NLS) fitting and a simplified reference tissue model (SRTM) were investigated for various noise levels and scan durations. In the human positron emission tomography (PET) study with and without antipsychotic, risperidone, the uncertainty of BP_{ND} and occupancy estimated by SRTM was investigated using resampled TACs based on bootstrap approach with weighted residual errors of fitting. For both NLS and SRTM, it was possible to have <3% of bias in occupancy estimates of [^{11}C]MNPA by 60 mins. However, shortened scan duration degrades the quantification of very small binding potentials, especially in case of SRTM. Observations were replicated on the clinical data. Results showed that dopamine D_2 receptor occupancy by antipsychotics can be estimated precisely in region of interest analysis by SRTM with a longer than 60-min [^{11}C]MNPA PET scan duration.
Journal of Cerebral Blood Flow & Metabolism (2010) **30,** 187–195; doi:10.1038/jcbfm.2009.193; published online 16 September 2009

Keywords: positron emission tomography; dopamine D_2 receptor; occupancy; [^{11}C]MNPA; bootstrap; reference region

Introduction

The dopamine D_2 receptor exists in both high- and low-affinity states, and the state of high affinity for endogenous dopamine is defined as the functionally active form of the receptor. To determine the binding to the high-affinity state of dopamine D_2 receptors, agonist ligands have been developed (Jones *et al*, 1984; Neumeyer *et al*, 1973). It has been reported that [^{11}C]-(R)-2-CH_3O-*N*-*n*-propylnorapomorphine ([^{11}C]MNPA), one of the agonist radioligands, is more sensitive than conventional D_2 antagonist radioligands [^{11}C]raclopride to the displacement of binding by endogenous dopamine, thus proposing [^{11}C]MNPA as promising radioligand for positron emission tomography (PET) imaging of the high-affinity state of dopamine D_2 receptors in the primate brain (Seneca *et al*, 2006).

The dopamine D_2 receptor is a main therapeutic target in schizophrenia, and most antipsychotics have an antagonistic action toward dopamine D_2 receptors. Occupancy of dopamine D_2 receptors evoked by competition from antipsychotic medication can be estimated from the reduction in the observed binding potential (BP_{ND}) (Farde *et al*, 1988; Farde *et al*, 1990). Several quantitative methods have been proposed for estimating BP_{ND}, and a simplified

Correspondence: Dr H Ito, Molecular Neuroimaging Group, Molecular Imaging Center, National Institute of Radiological Sciences, Anagawa 4-9-1, Inage, Chiba 263-8555, Japan.
E-mail: hito@nirs.go.jp
Received 27 May 2009; revised 10 August 2009; accepted 11 August 2009; published online 16 September 2009

reference tissue model (SRTM) (Lammertsma and Hume, 1996) has often been used. The SRTM uses as input the time activity of a reference brain region with negligible specific binding and therefore avoids arterial blood sampling. As an occupancy study requires two PET scans, elimination of arterial blood sampling by SRTM method has practical appeal.

Otsuka *et al* (2009) showed that the SRTM method can be applied to human [^{11}C]MNPA for quantitative BP_{ND} estimation; however, a precise quantitative evaluation of the SRTM method for occupancy studies with [^{11}C]MNPA has not yet been performed. However, error analysis is important to ascertain whether the variability in occupancy with antipsychotics measured [^{11}C]MNPA is truly biological or generated by the PET measurement system. In this regard, Yokoi *et al* reported that occupancy levels of the partial agonist aripiprazole, a new antipsychotic a partial agonist for dopamine D_2 receptors without notable extrapyramidal side effects, vary widely, contrasting with the usual presence of extrapyramidal side effects at occupancy levels exceeding 80% for D_2 antagonists (Farde *et al*, 1988; Kessler, 2007; Yokoi *et al*, 2002). It is therefore of relevance to perform an error analysis of BP_{ND} estimation for PET dynamic scanning with [^{11}C]MNPA to quantify the variability induced by the measurement itself to better appreciate the biological variability that may emerge from human bioassays that use this tracer.

In this study, we simulated and evaluated errors in the quantitative analysis for the estimation of dopamine D_2 receptor occupancy when measured with [^{11}C]MNPA with particular attention to the use of SRTM. The effect of scan duration on the error of estimates was also evaluated, because shorter scan duration reduces patient's burden. Tissue kinetics where simulated using a compartmental model and, to assess model validity, we compared the results of the simulations with the errors obtained from clinical data by use of a resampling technique.

Materials and methods

Kinetics of [^{11}C]MNPA

The kinetics of [^{11}C]MNPA in the brain is based on the two-tissue three-compartment model as follows:

$$\begin{aligned}\frac{dC_{ND}(t)}{dt} &= K_1 C_P(t) - (k_2 + k_3)C_{ND}(t) + k_4 C_S(t)\\ \frac{dC_S(t)}{dt} &= k_3 C_{ND}(t) - k_4 C_S(t)\\ C_T(t) &= C_{ND}(t) + C_S(t)\end{aligned} \quad (1)$$

where C_P [Bq/mL] is the radioactivity concentration of unchanged radioligand in plasma (arterial input function), C_{ND} [Bq/cm^3] is the radioactivity concentration of nondisplaceable radioligand in brain, including nonspecifically bound and free radioligand, and C_S [Bq/cm^3] is the radioactivity concentration of radioligand specifically bound to receptors. The rate constants K_1 [mL/cm^3/min] and k_2 [min^{-1}] represent the influx and efflux rates for radioligand diffusion through the blood–brain barrier. The rate constants k_3 [min^{-1}] and k_4 [min^{-1}] represent the radioligand transfers between the compartments for nondisplaceable and specifically bound radioligand. C_T [Bq/cm^3] is the radioactivity concentration in a brain region measured by PET.

Estimation of receptor occupancy

Nonlinear least squares fitting for BP_{ND}: K_1, k_2, k_3, and k_4 values in Equation (1) can be determined by nonlinear least squares (NLS) fitting of the time–activity curve (TAC) in the target region. The cerebellum is regarded as a reference region because this brain structure has negligible D_2 dopamine receptor density (Otsuka *et al*, 2009; Seneca *et al*, 2008; Tokunaga *et al*, 2009). K_1^r and k_2^r values in the cerebellum were also determined by NLS using the one-tissue compartment model without the specific binding compartment. The BP_{ND} can be expressed using the reference region as:

$$BP_{ND} = \frac{(K_1/k_2)(k_3/k_4 + 1)}{(K_1^r/k_2^r)} - 1 \quad (2)$$

where $(K_1/k_2)(k_3/k_4 + 1)$ is the total distribution volume of the target region and (K_1^r/k_2^r) is that of the cerebellum. In this study, the calculation of BP_{ND} in Equation (2) was regarded as the standard method for BP_{ND} estimation (Otsuka *et al*, 2009). It should be noted that to improve the stability of the NLS fitting for target regions, the K_1/k_2 ratio for the target region was assumed to be the value in the cerebellum (K_1^r/k_2^r) as obtained by NLS using the one-tissue compartment model, meaning that, as a result, BP_{ND} in Equation (2) is equivalent to k_3/k_4 in this study.

Simplified reference tissue model for BP_{ND}: The SRTM yields the binding potential value by eliminating the arterial input function, C_P, arithmetically from model equations by using a TAC from a reference region where specific bindings are negligible, under the assumptions that the distribution volume of the nondisplaceable compartment was equal in the target and reference regions, and that a target region can be described with the one-tissue compartment model shown in Equation (3) (Lammertsma and Hume, 1996).

$$\begin{aligned}C_T(t) &= R_1 \cdot C_R(t) + \left(k_2 - \frac{R_1 k_2}{1 + BP_{ND}}\right) \cdot e^{\left(-\frac{k_2}{1+BP_{ND}}t\right)} \otimes C_R(t)\\ R_1 &= K_1/K_1^r\end{aligned} \quad (3)$$

where C_T and C_R are the radioactivity concentrations in the target and reference regions, respectively. The SRTM estimates three parameters, the delivery ratio of the target region to reference region (R_1), the clearance rate constant of the target region (k_2), and binding potential, referred to as BP_{ND} by nonlinear least squares.

Receptor occupancy: Receptor occupancy is calculated from BP_{ND} of two scans, with and without antipsychotics, as follows:

$$Occupancy\ (\%) = 100 \cdot (BP_{control} - BP_{drug})/BP_{control} \quad (4)$$

where $BP_{control}$ represents the BP_{ND} value derived from a scan without drug and BP_{drug} represents that from a scan with drug (Farde *et al*, 1988).

Simulation study

To evaluate the dependency of the noise level and scan duration for the estimated BP_{ND} and occupancy, we performed the following simulations. Both NLS and SRTM procedures were performed using in-house software written in the C program with downhill simplex algorithm (Nelder and Mead, 1965) without weighting and without constraints for the range of estimated parameters.

Time–activity curves for [^{11}C]MNPA: A dynamic tracer concentration for [^{11}C]MNPA was derived from the kinetic parameters listed in Table 1 with a dynamic frame (20 secs × 9, 1 min × 5, 2 mins × 4, 4 mins × 11, 5 mins × 6, total 90 mins) and a measured arterial input function (10 secs × 12, 30 secs × 2, 60 secs × 7, 120 secs × 1, 180 secs × 1, 300 secs × 3, 600 secs × 6, total 90 mins) of a single subject obtained by Otsuka *et al* (2009). These K_1, k_2, and k_4 were estimated based on the two-tissue three-compartment model using NLS fitting of region of interests (ROIs) in the putamen at baseline (the number of subjects (n) = 10) (Otsuka *et al*, 2009). Furthermore, three k_3 values, 0.015, 0.075, and 0.15, were arbitrarily chosen to investigate the occupancy of antipsychotics with [^{11}C]MNPA. During a loading study with a drug, the observed binding potential (BP_{ND}) is reduced mainly due to the suppression of the radioligand transfers from the compartments for nondisplaceable to specifically bound radioligand, k_3. Therefore, we varied k_3 values while covering the practical range of occupancy from a likely level at 50% to the extreme scenario of a 90% occupancy. A measured arterial plasma input function of a single subject according to human PET imaging protocols and noise-free simulated TACs (three target curves and a reference) are shown in Figure 1A and B.

Noise was generated with random generator based on Gaussian distribution and added to the decay-corrected target TACs. The noise ratio for each time frame was determined (Ikoma *et al*, 2008) according to the collected total count given by

$$NOISE_i(\%) = \left(\sqrt{N_i}/N_i\right) \cdot 100$$
$$N_i = \int_{t_i-\frac{\Delta t_i}{2}}^{t_i+\frac{\Delta t_i}{2}} C_T(t) \cdot e^{-\lambda t} dt \cdot F \quad (5)$$

where i is the frame number, C_T is the decay-corrected tissue radioactivity concentration derived from the k-values and the input function, t_i is the midpoint time of the i-th frame, Δt_i is the data collection time, λ is the radioisotope decay constant, and F is a scaling factor representing the sensitivity of the measurement system and is introduced here for adjusting the noise level.

Noise level dependency: Target TACs of [^{11}C]MNPA with several noise levels were generated to investigate the bias and variation of parameter estimates caused by the statistical noise for NLS and SRTM. The bias and variation were calculated as %bias of estimated BP_{ND} against the true BP_{ND} value and coefficient of variance (COV) by the mean and s.d. of the estimates excluding the outliers, respectively.

In this simulation study, the noise level for dynamic data was expressed as the mean of percentage noise described in Equation (5) from 1 to 90 mins, and it was chosen so that the mean of percentage noise would be 1%, 3%, 5%, 7%, and 10%, with 500 noisy data sets being generated for each. An example of noise-added simulated TAC with $BP_{ND} = 0.417$ is shown in Figure 1C.

In these noise-added TACs, each kinetic parameter including BP_{ND} was estimated by NLS and SRTM with a noise-free reference TAC. For both NLS and SRTM, initial parameters varied by ±25% from the true value (Ichise *et al*, 2003; Ikoma *et al*, 2008), and parameter estimates were considered invalid outliers if estimated parameters were negative or more than three times the true value (Ichise *et al*, 2003; Ikoma *et al*, 2008). Occupancy was also calculated from Equation (4) by using estimated BP_{ND} with assumed $k_3 = 0.15$ as $BP_{control}$ and with assumed $k_3 = 0.015$ or 0.075 as BP_{drug}.

Scan duration: The effect of scan duration on BP_{ND} and occupancy estimates was investigated for both NLS and SRTM methods. In the 90-min simulated TACs of 3% noise level corresponding to the noise level of human ROI analysis, the duration of the scan used for the parameter estimation was progressively reduced from 90 to 32 mins (32, 44, 60, 75, and 90 mins) for [^{11}C]MNPA.

Table 1 Kinetic parameters for the simulation study of [^{11}C]MNPA

	K_1	k_2	k_3	k_4	BP_{ND}	Occup. (%)
Target regions	0.44	0.067	0.015	0.18	0.0833	90
			0.075		0.417	50
			0.15		0.833	—
Reference region	0.44	0.067	—	—	—	—

Human study

Subjects and positron emission tomography procedure: [^{11}C]MNPA PET studies were performed before and after antipsychotic drug administration of risperidone (0.5 and 2.0 mg) on separate days for each two healthy male volunteers (20 to 21 y.o.). Scan start time after antipsychotic administration was 4 h. The study was approved by the ethics and radiation safety committees of the National

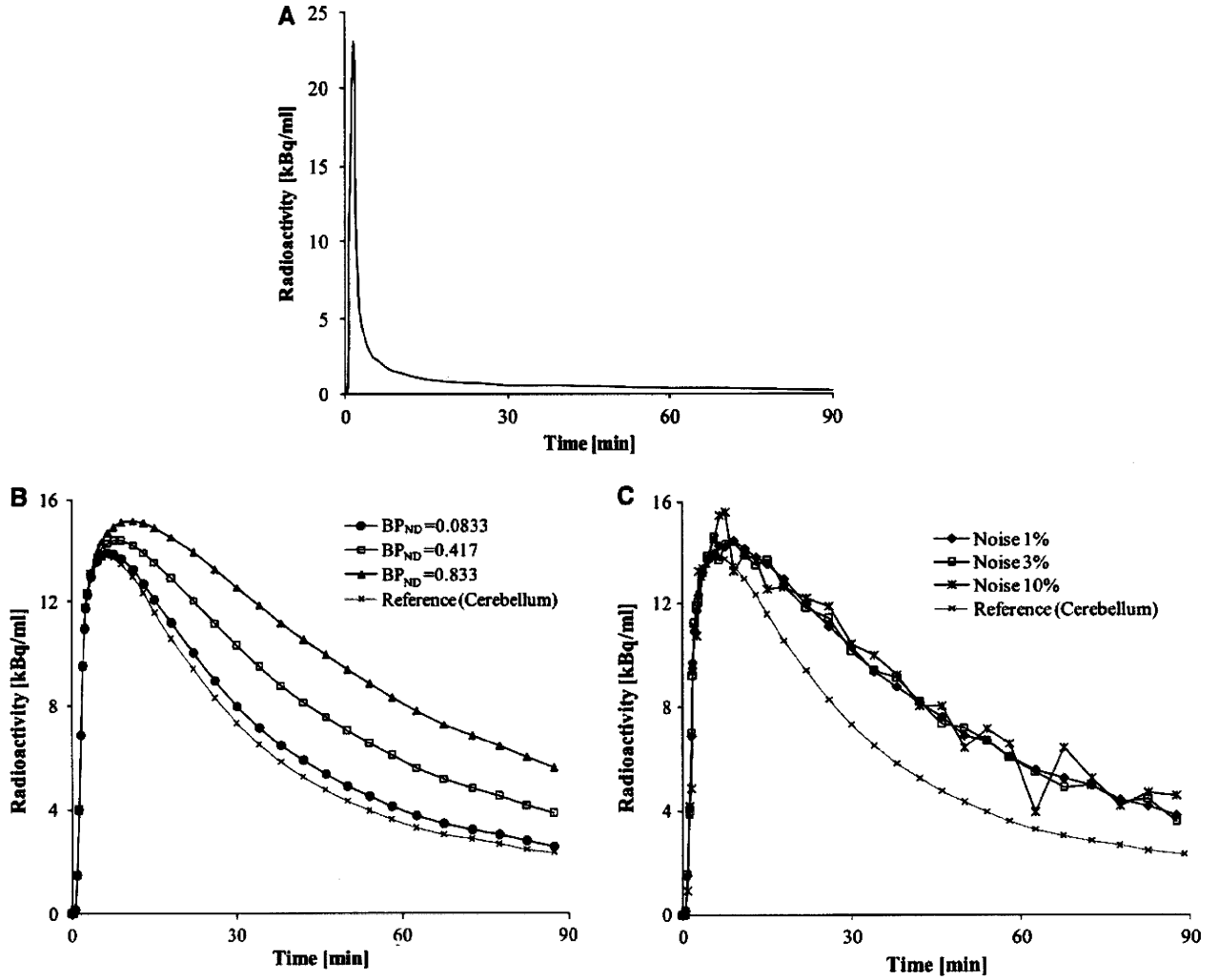

Figure 1 (**A**) Metabolite-corrected plasma input function of a single normal subject for simulation study. (**B**) Noise-free simulated TACs of three BP_{ND} values and reference TAC. (**C**) Noise-added TACs in the case of $BP_{ND} = 0.417$.

Institute of Radiological Sciences, Chiba, Japan. Written informed consent was obtained from each subject.

The PET acquisitions were performed on the ECAT EXACT HR+ (CTI-Siemens, Knoxville, TN, USA). A 10-min transmission scan with 3-rod source of ^{68}Ge–^{68}Ga was performed. Dynamic PET scans of [^{11}C]MNPA were performed for 90 mins in three-dimensional mode with a bolus injection of 208.0 to 234.0 MBq. Frame intervals were the same as this simulation study. The specific radioactivity was 245.1 to 313.8 GBq/μmol at the time of injection. Arterial blood sampling was not performed. All emission data were reconstructed by filtered-back projection using a Hanning filter with a cut-off frequency of 0.4.

Data analysis: The summed PET images for all frames were coregistered to individual MR images, and ROIs were drawn manually over the putamen, caudate, and cerebellum. Especially, R_1, k_2, and BP_{ND} in the putamen were estimated by SRTM using the cerebellum as reference region.

Human data were used to check model validity for the simulation studies. Given that an occupancy is measured only once (two scans for subject) and that repetitive measurements are not usually available, the reliability of parameter estimates can be evaluated by a bootstrap approach with weighted residual errors of fitting as published earlier (Rosso *et al*, 2009; Turkheimer *et al*, 1998). For each ROI in each individual subject data, 500 replication TACs were generated using bootstrap approach, and then parameters were estimated by SRTM and the COV of these 500 estimates was calculated to produce an accurate estimate of the statistical variability of the parameters. The weighted residual, ξ, using model-predicted tissue TAC, C_T, and the measured tissue TAC, X, were calculated as follows;

$$\xi_i = (X(t_i) - C_T(t_i)) \cdot \sqrt{N_i}$$
$$N_i = \int_{t_i - \frac{\Delta t_i}{2}}^{t_i + \frac{\Delta t_i}{2}} C_T(t) \cdot e^{-\lambda t} dt \qquad (6)$$

Then the residuals, $\{\xi_i\}$ $(i = 1, \ldots, k)$, were randomly resampled with substitution into a new set of the residuals

$\{\xi_i^*\}$. As an example with $k=5$, $[\xi_1, \xi_2, \xi_3, \xi_4, \xi_5]$ were randomly selected $[\xi_5, \xi_1, \xi_4, \xi_1, \xi_3]$ as a new residual set $[\xi_1^*, \xi_2^*, \xi_3^*, \xi_4^*, \xi_5^*]$. The bootstrapped residuals were used to generate a new data X^* defined as,

$$X^*(t_i) = C_T(t_i) + \frac{\xi_i^*}{\sqrt{N_i}} \quad (7)$$

In keeping with the simulation study, the relationship between the scan duration and COV of estimates and between the scan duration and bias was investigated by shortening the interval of fitting of the bootstrap replication TACs from 90 to 32 mins. The bias of BP_{ND} and occupancy was defined as the difference between the mean of these calculated for each truncated fitting interval and that of the 90 mins. Parameter estimates based on bootstrap approach were considered invalid outliers if estimates from X^* were negative or more than three times that of the 90 mins.

Results

Simulation study

Noise level dependency: In the NLS method, the bias of BP_{ND} was small especially at a low noise level. However, COV of BP_{ND} became larger as the noise level increased (Figure 2A). In the SRTM method, the bias of BP_{ND} was observed even though TACs were free from noise and both the bias and COV of BP_{ND} became larger as the noise increased, which is typical in the case of small BP_{ND} (Figure 2B). For both NLS and SRTM methods, these bias and COV values of occupancy were smaller compared with BP_{ND}. The tendency that COV with 90% occupancy was smaller compared with that with 50% occupancy was a common observation for NLS and SRTM.

Scan duration: The relationship between the reliability of BP_{ND} and occupancy estimates and the scan duration was investigated as shown in Figure 3. The bias of BP_{ND} and occupancy estimated by NLS was small despite short scan durations (Figure 3A); however, more than 10% outliers was caused with $BP_{ND}=0.0833$ at 32, 44, 60, 75, and 90 mins (Table 2). As scanning time became shorter, BP_{ND} for all three conditions was overestimated by SRTM (Figure 3B) and its bias magnitude was larger than that of NLS. More than 10% outliers was seen with $BP_{ND}=0.0833$ at 32 and 44 mins, $BP_{ND}=0.417$ at 32 mins and 0.833 at 32 mins. Bias was under 3% at a 3% noise level with occupancy estimates by SRTM method with scan duration longer than 60 mins (Figure 3B).

Human study

Time–activity curves: As shown in Figure 4, the shape of the TACs was similar between before and after antipsychotic administration in the cerebellum, whereas the accumulation of radioactivity in the postantipsychotic scan decreased at late times in other regions. In Figure 4A and B, estimated BP_{ND} in putamen of a subject before and after administration of Risperidone 2 mg were 0.968 and 0.437, then its occupancy resulted in 54.8%. For the other subject shown in Figure 4C and D, estimated BP_{ND} in putamen of a subject before and after administration

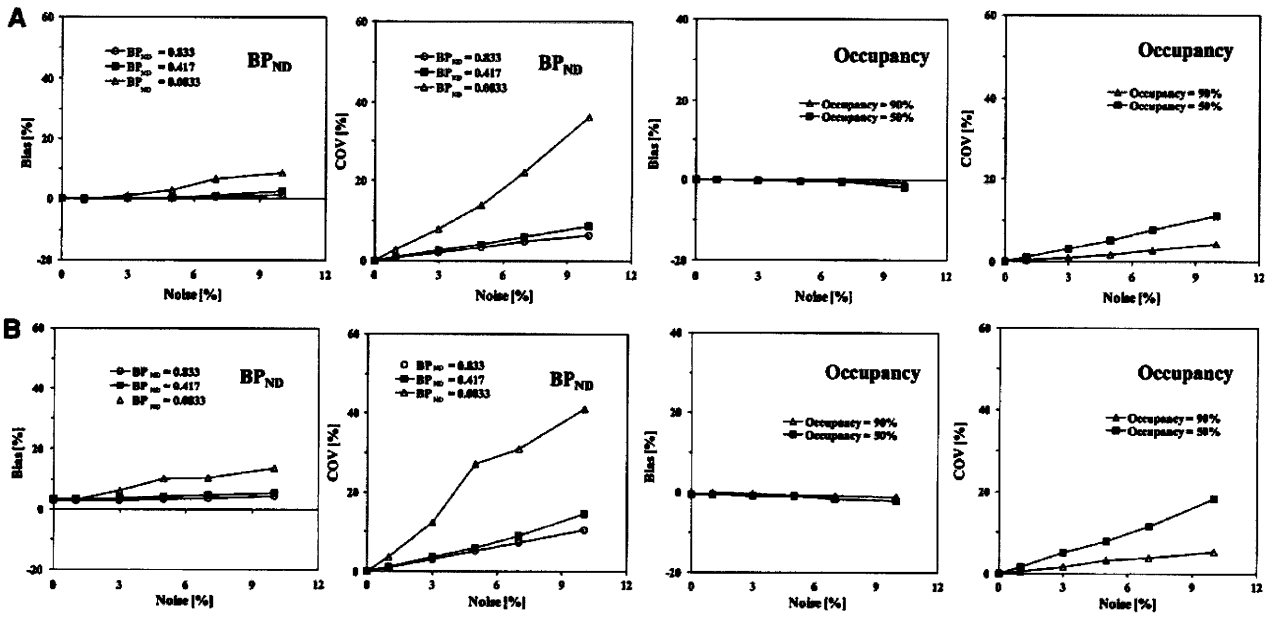

Figure 2 Noise level dependency. (**A**) Bias and COV of BP_{ND} and occupancy estimated by NLS ($K_1/k_2 = 6.6$ fixed), (**B**) estimated by SRTM.

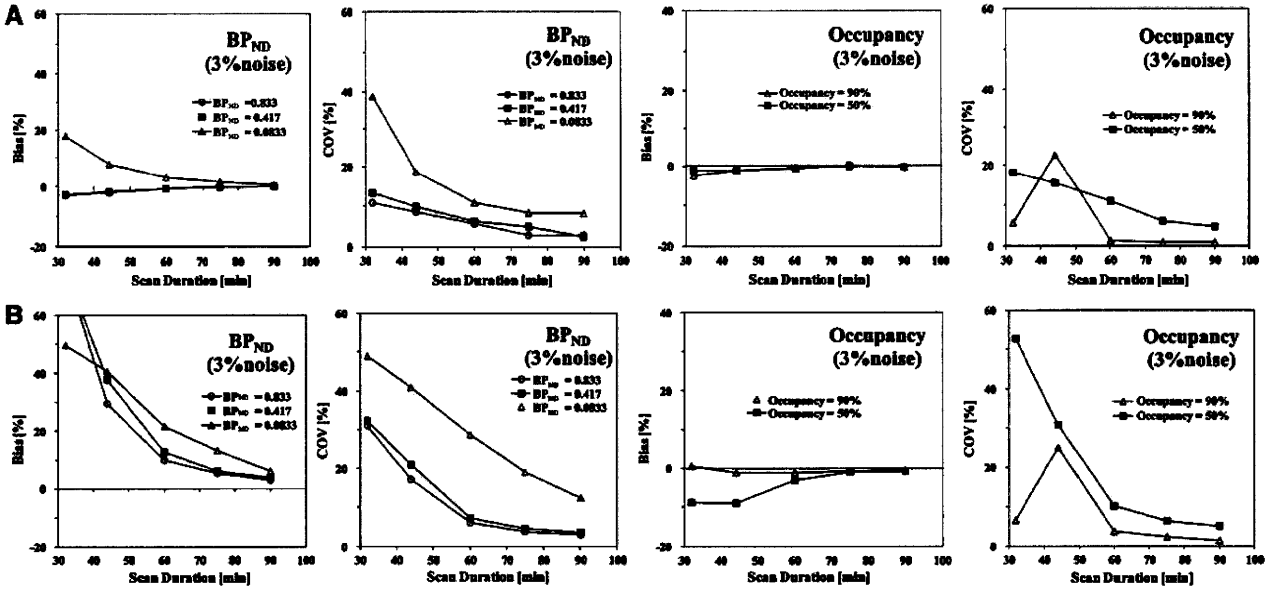

Figure 3 Scan duration dependency of bias and COV of BP_{ND} and occupancy at a 3% noise level estimated by (**A**) NLS and (**B**) SRTM methods.

Table 2 Scan duration dependency on the percentages of outliers of BP_{ND} at 3% noise level estimated by NLS and SRTM

	BP_{ND}	*Scan duration (min)*				
		32	*44*	*60*	*75*	*90*
NLS	0.0833	27.4	22.8	22.6	12.8	10.8
	0.417	5.8	3.4	1.4	2.6	1.2
	0.833	3.8	1.8	0.2	0	0
SRTM	0.0833	40.4	19.8	3.4	0.2	0
	0.417	29.2	0.6	0	0	0
	0.833	26.0	0.2	0	0	0

NLS, nonlinear least square; SRTM, simplified reference tissue model.

of Risperidone 0.5 mg were 0.866 and 0.496, then its occupancy resulted in 42.7%.

Scan duration: On the basis of the bootstrap approach, the relationship between the reliability of BP_{ND} and occupancy estimates and the scan duration was investigated as shown in Figure 5.

As scanning time became shorter, BP_{ND} in both before and after antipsychotics administration for two volunteers was overestimated. However, the bias of occupancy was small despite short scan durations. The COVs of both BP_{ND} and occupancy also became larger with shorter scan durations. These observations are consistent with the simulation results especially in the case of occupancy shown in Figure 3B, even though a small difference of magnitude of bias in BP_{ND} was still observed.

Discussion

In this study, we evaluated the effect of noise and scan duration of dynamic PET [^{11}C]MNPA studies on the BP_{ND} estimates obtained with NLS and SRTM for a range of BP_{ND} values, a range that is likely to be encountered in occupancy studies with antipsychotic medication. Error analysis was performed using artificial datasets. The validity of the simulations was assessed by using the bootstrap on a small cohort of human data to calculate 'real variances' that resulted in good agreement with those obtained from the artificial datasets.

Reliability of estimated parameters

In the case of NLS, the larger number of parameters introduced instability and, even though we introduced a fixed K_1/k_2 ratio, the variability of BP_{ND} was still significant as shown by the percentage of outliers by NLS (Table 2). K_1/k_2 for both target and reference regions were same in this simulation study; however, in clinical situation, sometimes K_1/k_2 values may vary from regions to regions (Ginovart *et al*, 2007) and these difference may introduce errors in BP_{ND} when the ratio K_1/k_2 is fixed.

The SRTM provided reliable estimates although variability increased for low BP_{ND} values even with favorable noise levels (Gunn *et al*, 1997; Ikoma *et al*, 2008). As shown in Figure 2B, both bias and COV with small $BP_{ND} = 0.0833$ were larger than those with $BP_{ND} = 0.417$ or 0.833. The small bias of BP_{ND} estimates in noise-free TACs (Figure 2B) may originate from the two-tissue model of the target

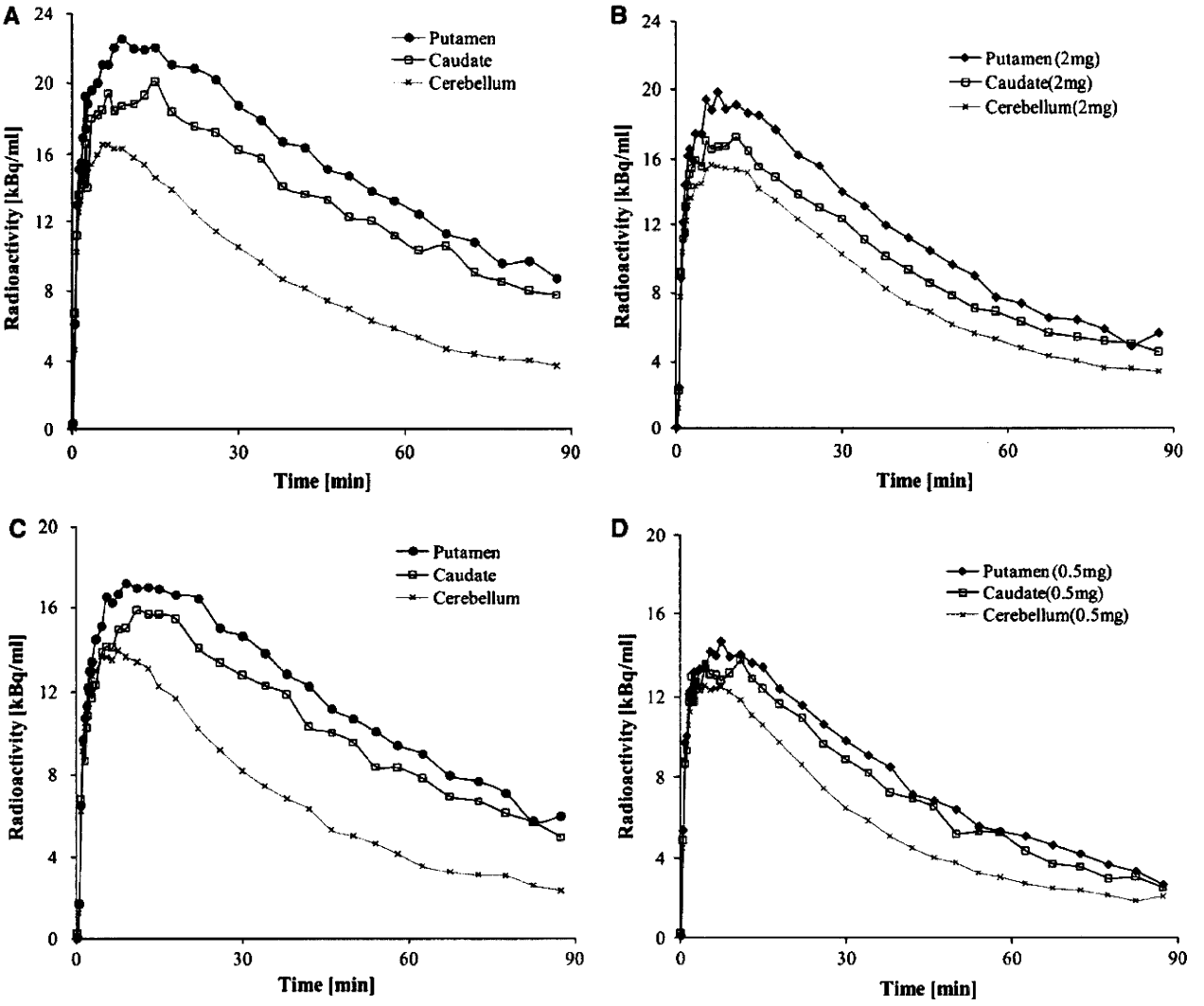

Figure 4 TACs for a single subject with baseline (**A**), and 2 mg administration of Risperidone (**B**), TAC for the other subject with baseline (**C**), and 0.5 mg administration of Risperidone (**D**). ROIs were drawn on putamen, caudate, and cerebellum.

tissue. In the SRTM method, even when the one-tissue model for target tissue is not appropriate, the apparent rate constant ($=k_2/(1+BP_{ND})$ in Equation (3) could be used to fit the curves well and bias in BP_{ND} is negligible (Wu and Carson, 2002). In this study, as shown in Figure 2B, the bias of BP_{ND} was small and the error propagation of biased BP_{ND} to occupancy in the SRTM method was also small. Errors of both estimated BP_{ND} and occupancy by SRTM were small at a low noise level, indicating that ROI analysis of SRTM will be useful for a quantified BP_{ND} and occupancy study with [^{11}C]MNPA.

In the simulation study, the reference TAC was assumed as noise free; however, noise may affect the reference TAC depending on the size of ROI (Ogden and Tarpey, 2006). For SRTM, the use of a 1% noise on the reference TAC increased %COV of the BP_{ND} estimates for the target regions (where noise was 3%) by 20% to 30%. However, the noise in the reference TAC did not change the profile of BP_{ND} %COV in the target TAC according to scan duration nor changed the biases in the estimated occupancies that remained similar.

Effects of scan duration

In the simulation study, a 60-min scan duration gave unbiased and reliable BP_{ND} and occupancy estimates by NLS with [^{11}C]MNPA both at baseline and with drug load (Figure 3A). Conversely, the results of SRTM method showed that at least 60-min scan duration would be required for the quantification of occupancy; bias was under 3% at a 3% noise level with scan duration longer than 60 mins (Figure 3B). Shorter scan duration caused larger bias of BP_{ND} estimated by SRTM. Note that the sampling rate of the reference input function is inherently lower than

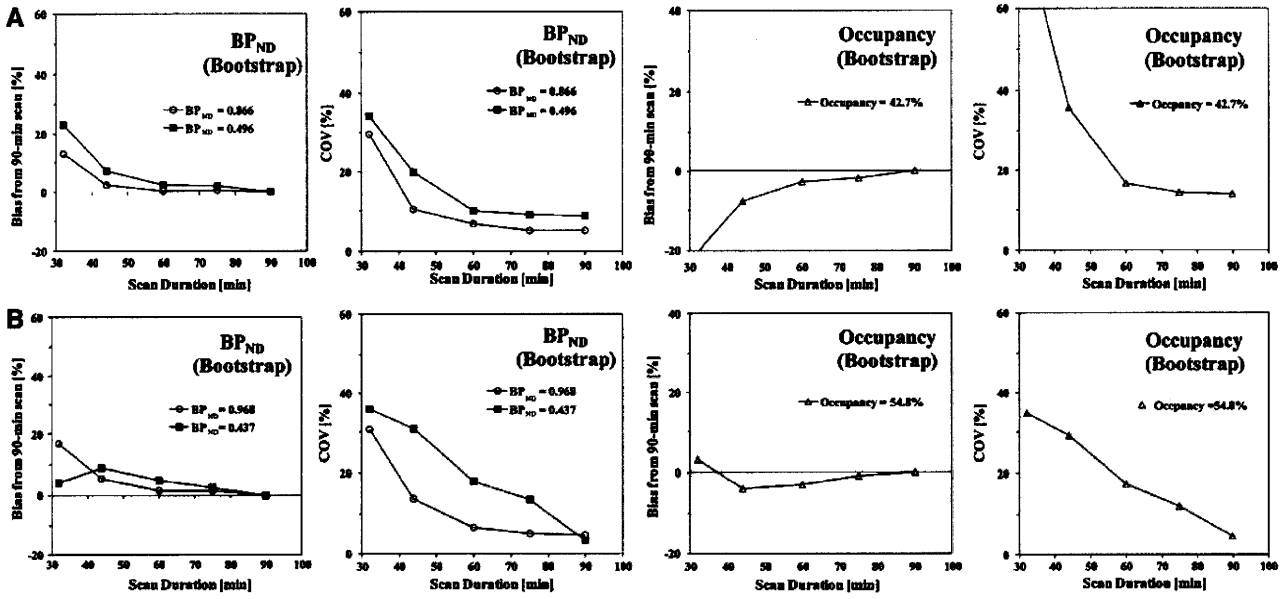

Figure 5 Scan duration dependency of bias and COV of BP_{ND} and occupancy in the putamen estimated by SRTM method for a single subject with 0.5 mg administration (**A**) and the other subject with 2 mg administration (**B**).

the one of the plasma input function and this may introduce errors with SRTM although in this instance, kinetics in tissue are not particularly fast.

The use of the bootstrap approach on clinical data validated most of the observations obtained from simulations for the SRTM method, such as the overestimation of BP_{ND} and underestimation of occupancy at shorter scan durations. It is important to remark that the variability considered here is the one associated with the measurement error only. Further variability of biological origin (between subjects and/or associated with age, gender, etc. (Inoue *et al*, 2001; Kaasinen *et al*, 2001)) should be taken into account and possibly controlled at the design stage.

We can therefore conclude that, for both NLS and SRTM methods, reliable and unbiased occupancy estimates of [^{11}C]MNPA could be obtained by 60 mins, with COV of 50% occupancy remaining at 11.0% and 10.1%, respectively (Figure 3). In the case of lower occupancy than 50%, COV at 60-min scan duration may be >11% but no bias should be expected.

Conclusion

The effects of bias, variance, and scan duration in PET quantitative analysis of dopamine D_2 receptor occupancy using [^{11}C]MNPA were evaluated in a simulation study and validated using a bootstrap approach on clinical data. The results suggest that a reference approach with SRTM applied to ROI data with a scan duration of at least 60-mins PET scan duration represent a valid bioassay for the task.

Acknowledgements

This study was supported in part by Grants-in-Aid for Young Scientists (B) (No. 19700395) and by a consignment expense for the Molecular Imaging Program on 'Research Base for PET Diagnosis' from the Ministry of Education, Culture, Sports, Science and Technology (MEXT), Japanese Government and by the Royal Society, International Project Grant no. JP0871550, UK. We thank Dr Hiroshi Watabe for his valuable advice.

Conflict of interest

The authors declare no conflict of interest.

References

Farde L, Wiesel FA, Halldin C, Sedvall G (1988) Central D2-dopamine receptor occupancy in schizophrenic patients treated with antipsychotic drugs. *Arch Gen Psychiatry* 45:71–6

Farde L, Wiesel FA, Stone-Elander S, Halldin C, Nordstrom AL, Hall H, Sedvall G (1990) D2 dopamine receptors in neuroleptic-naive schizophrenic patients. A positron emission tomography study with [11C]raclopride. *Arch Gen Psychiatry* 47:213–9

Ginovart N, Willeit M, Rusjan P, Graff A, Bloomfield PM, Houle S, Kapur S, Wilson AA (2007) Positron emission tomography quantification of [11C]-(+)-PHNO binding in the human brain. *J Cereb Blood Flow Metab* 27:857–71

Gunn RN, Lammertsma AA, Hume SP, Cunningham VJ (1997) Parametric imaging of ligand-receptor binding in PET using a simplified reference region model. *Neuroimage* 6:279–87

Ichise M, Liow JS, Lu JQ, Takano A, Model K, Toyama H, Suhara T, Suzuki K, Innis RB, Carson RE (2003) Linearized reference tissue parametric imaging methods: application to [11C]DASB positron emission tomography studies of the serotonin transporter in human brain. *J Cereb Blood Flow Metab* 23:1096–112

Ikoma Y, Ito H, Arakawa R, Okumura M, Seki C, Shidahara M, Takahashi H, Kimura Y, Kanno I, Suhara T (2008) Error analysis for PET measurement of dopamine D2 receptor occupancy by antipsychotics with [11C]raclopride and [11C]FLB 457. *Neuroimage* 42:1285–94

Inoue M, Suhara T, Sudo Y, Okubo Y, Yasuno F, Kishimoto T, Yoshikawa K, Tanada S (2001) Age-related reduction of extrastriatal dopamine D2 receptor measured by PET. *Life Sci* 69:1079–84

Jones JH, Anderson PS, Baldwin JJ, Clineschmidt BV, McClure DE, Lundell GF, Randall WC, Martin GE, Williams M, Hirshfield JM *et al* (1984) Synthesis of 4-substituted 2H-naphth[1,2-b]-1,4-oxazines, a new class of dopamine agonists. *J Med Chem* 27:1607–13

Kaasinen V, Nagren K, Hietala J, Farde L, Rinne JO (2001) Sex differences in extrastriatal dopamine d(2)-like receptors in the human brain. *Am J Psychiatry* 158:308–11

Kessler RM (2007) Aripiprazole: what is the role of dopamine D(2) receptor partial agonism? *Am J Psychiatry* 164:1310–2

Lammertsma AA, Hume SP (1996) Simplified reference tissue model for PET receptor studies. *Neuroimage* 4:153–8

Nelder JA, Mead R (1965) A simplex method for function minimization. *Comput J* 7:308–13

Neumeyer JL, Neustadt BR, Oh KH, Weinhardt KK, Boyce CB, Rosenberg FJ, Teiger DG (1973) Aporphines. 8. Total synthesis and pharmacological evaluation of (plus or minus)-apomorphine, (plus or minus)-apocodeine, (plus or minus)-N-n-propylnorapomorphine, and (plus or minus)-N-n-propylnorapocodeine. *J Med Chem* 16:1223–8

Ogden RT, Tarpey T (2006) Estimation in regression models with externally estimated parameters. *Biostatistics* 7:115–29

Otsuka T, Ito H, Halldin C, Takahashi H, Takano H, Arakawa R, Okumura M, Kodaka F, Miyoshi M, Sekine M, Seki C, Nakao R, Suzuki K, Finnema SJ, Hirayama Y, Suhara T, Farde L (2009) Quantitative PET analysis of the dopamine D2 receptor agonist radioligand 11C-(R)-2-CH3O-N-n-propylnorapomorphine in the human brain. *J Nucl Med* 50:703–10

Rosso L, Brock CS, Gallo JM, Saleem A, Price PM, Turkheimer FE, Aboagye EO (2009) A new model for prediction of drug distribution in tumor and normal tissues: pharmacokinetics of temozolomide in glioma patients. *Cancer Res* 69:120–7

Seneca N, Finnema SJ, Farde L, Gulyas B, Wikstrom HV, Halldin C, Innis RB (2006) Effect of amphetamine on dopamine D2 receptor binding in nonhuman primate brain: a comparison of the agonist radioligand [^{11}C]MNPA and antagonist [^{11}C]raclopride. *Synapse* 59:260–9

Seneca N, Skinbjerg M, Zoghbi SS, Liow JS, Gladding RL, Hong J, Kannan P, Tuan E, Sibley DR, Halldin C, Pike VW, Innis RB (2008) Kinetic brain analysis and whole-body imaging in monkey of [^{11}C]MNPA: a dopamine agonist radioligand. *Synapse* 62:700–9

Tokunaga M, Seneca N, Shin RM, Maeda J, Obayashi S, Okauchi T, Nagai Y, Zhang MR, Nakao R, Ito H, Innis RB, Halldin C, Suzuki K, Higuchi M, Suhara T (2009) Neuroimaging and physiological evidence for involvement of glutamatergic transmission in regulation of the striatal dopaminergic system. *J Neurosci* 29: 1887–96

Turkheimer F, Sokoloff L, Bertoldo A, Lucignani G, Reivich M, Jaggi JL, Schmidt K (1998) Estimation of component and parameter distributions in spectral analysis. *J Cereb Blood Flow Metab* 18:1211–22

Wu Y, Carson RE (2002) Noise reduction in the simplified reference tissue model for neuroreceptor functional imaging. *J Cereb Blood Flow Metab* 22:1440–52

Yokoi F, Grunder G, Biziere K, Stephane M, Dogan AS, Dannals RF, Ravert H, Suri A, Bramer S, Wong DF (2002) Dopamine D2 and D3 receptor occupancy in normal humans treated with the antipsychotic drug aripiprazole (OPC 14597): a study using positron emission tomography and [11C]raclopride. *Neuropsychopharmacology* 27:248–59

Behavioral/Systems/Cognitive

Dopamine D_1 Receptors and Nonlinear Probability Weighting in Risky Choice

Hidehiko Takahashi,[1,2,3,4] Hiroshi Matsui,[2] Colin Camerer,[5] Harumasa Takano,[2] Fumitoshi Kodaka,[2] Takashi Ideno,[6] Shigetaka Okubo,[6] Kazuhisa Takemura,[6] Ryosuke Arakawa,[2] Yoko Eguchi,[2] Toshiya Murai,[1] Yoshiro Okubo,[7] Motoichiro Kato,[8] Hiroshi Ito,[2] and Tetsuya Suhara[2]

[1]Department of Psychiatry, Kyoto University Graduate School of Medicine, Kyoto, 606-8507, Japan, [2]Molecular Imaging Center, Department of Molecular Neuroimaging, National Institute of Radiological Sciences, Chiba, 263-8555, Japan, [3]Precursory Research for Embryonic Science and Technology (PRESTO), Japan Science and Technology Agency, Saitama, 332-0012, Japan, [4]Brain Science Institute, Tamagawa University, Tokyo, 194-8610, Japan, [5]Division of Humanities and Social Sciences, California Institute of Technology, Pasadena, California 91125, [6]Department of Psychology, Waseda University, Tokyo, 162-8644, Japan, [7]Department of Neuropsychiatry, Nippon Medical School, Tokyo 113-8603, Japan, and [8]Department of Neuropsychiatry, Keio University School of Medicine, Tokyo 160-8582, Japan

Misestimating risk could lead to disadvantaged choices such as initiation of drug use (or gambling) and transition to regular drug use (or gambling). Although the normative theory in decision-making under risks assumes that people typically take the probability-weighted expectation over possible utilities, experimental studies of choices among risks suggest that outcome probabilities are transformed nonlinearly into subjective decision weights by a nonlinear weighting function that overweights low probabilities and underweights high probabilities. Recent studies have revealed the neurocognitive mechanism of decision-making under risk. However, the role of modulatory neurotransmission in this process remains unclear. Using positron emission tomography, we directly investigated whether dopamine D_1 and D_2 receptors in the brain are associated with transformation of probabilities into decision weights in healthy volunteers. The binding of striatal D_1 receptors is negatively correlated with the degree of nonlinearity of weighting function. Individuals with lower striatal D_1 receptor density showed more pronounced overestimation of low probabilities and underestimation of high probabilities. This finding should contribute to a better understanding of the molecular mechanism of risky choice, and extreme or impaired decision-making observed in drug and gambling addiction.

Introduction

Life is filled with risks. Should I take an umbrella with me this morning? Should I buy car insurance? Which therapy or medicine will improve my health? To answer these questions, and choose, weighting the probability of the possible outcomes is crucial. In particular, misestimating risk could lead to disadvantaged choices such as initiation of drug use (or gambling) and transition to regular drug use (or gambling) (Kreek et al., 2005).

Normative theory in decision-making under risks assumes that people combine probabilities and valuation (utility) of possible outcomes in some way, most typically by taking the probability-weighted expectation over possible utilities. While this expected utility theory (von Neumann and Morgenstern, 1944) is the dominant model, a substantial body of evidence shows that decision makers systematically depart from it (Camerer and Loewenstein, 2004). One type of systematic departure is that subjective weights on probabilities appear to be nonlinear: people often overestimate low probabilities (e.g., playing lotteries) and underestimate high probabilities.

A leading alternative to the expected utility theory is the prospect theory (Tversky and Kahneman, 1992). In the prospect theory, objective probabilities, p, are transformed nonlinearly into decision weights $w(p)$ by a weighting function. Experimental estimates suggest the weighting function is regressive, asymmetric, and inverse S-shaped, crossing the diagonal from above at an inflection point (about 1/3) where $p = w(p)$. In an inverse S-shaped nonlinear weighting function, low probabilities are overweighted and moderate to high probabilities are underweighted. The function neatly explains the typically observed pattern of risk-seeking for low probability gain and risk aversion toward high probability gain.

Risky choice is one of the topics explored in a synthesis of economics and neuroscience called neuroeconomics. Neuroeconomics fMRI studies have demonstrated the neural basis for some other features of the prospect theory such as framing effects and loss aversion (De Martino et al., 2006; Tom et al., 2007). Recently, the neural basis for nonlinear weighting function has also been investigated by fMRI. Hsu et al. (2009) reported that the degree of nonlinearity in the neural response to anticipated re-

Received July 28, 2010; revised Sept. 12, 2010; accepted Oct. 8, 2010.

This study was supported by a consignment expense for Molecular Imaging Program on "Research Base for PET Diagnosis" from the Ministry of Education, Culture, Sports, Science and Technology (MEXT). We thank Katsuyuki Tanimoto and Takahiro Shiraishi for their assistance in performing the PET experiments at the National Institute of Radiological Sciences. We also thank Yoshiko Fukushima of the National Institute of Radiological Sciences for her help as clinical research coordinator.

Correspondence should be addressed to Dr. Hidehiko Takahashi, Department of Psychiatry, Kyoto University Graduate School of Medicine, 54 Shogoin-Kawara-cho, Sakyo-ku, Kyoto, 606-8507, Japan. E-mail: hidehiko@kuhp.kyoto-u.ac.jp.

DOI:10.1523/JNEUROSCI.3933-10.2010

 0270-6474/10/3016567-06$15.00/0

ward in the striatum reflected the nonlinearity parameter as estimated behaviorally.

A deeper question is how modulatory neurotransmission is involved in the central process of decision-making (Trepel et al., 2005; Rangel et al., 2008; Fox and Poldrack, 2009). Investigation of the relationship between the dopamine (DA) system and prospect theory seems promising, considering the fact that DA is linked to risk-seeking behavior (Leyton et al., 2002) and is involved in disrupted decision-making observed in neuropsychiatric disorders such as drug/gambling addiction and Parkinson's disease (Zack and Poulos, 2004; Steeves et al., 2009). Trepel et al. (2005) speculated in a thoughtful review that DA transmission in the striatum might be involved in shaping probability weighting. Using positron emission tomography (PET), we tested this speculation directly by investigating how DA D_1 and D_2 receptors in the brain are associated with transformation of probabilities into decision weights. Phasic DA release occurs during reward and reward-predicting stimuli (Grace, 1991; Schultz, 2007). It is suggested that available striatal D_1 receptors are preferentially stimulated by phasically released DA, whereas low-level baseline tonic DA release is enough for stimulating striatal D_2 receptors (Frank et al., 2007; Schultz, 2007). Because estimating reward cue in our task is considered to induce phasic DA release, we hypothesized that the variability of available D_1 receptors might be more associated with individual differences than that of available D_2 receptors.

Materials and Methods

Subjects

Thirty-six healthy male volunteers (mean age ± SD, 25.2 ± 4.9 years) were studied. They did not meet the criteria for any psychiatric disorder based on unstructured psychiatric screening interviews. None of the controls were taking alcohol at the time, nor did they have a history of psychiatric disorder, significant physical illness, head injury, neurological disorder, or alcohol or drug dependence. Ten subjects were light to moderate cigarette smokers. All subjects were right-handed according to the Edinburgh Handedness Inventory. The vast majority of subjects were university students or graduate school students (three of the participants had finished university and were employed). All subjects underwent MRI to rule out cerebral anatomic abnormalities. After complete explanation of the study, written informed consent was obtained from all subjects, and the study was approved by the Ethics and Radiation Safety Committee of the National Institute of Radiological Sciences, Chiba, Japan.

Procedure

To estimate decision weight, certainty equivalents were determined outside the PET scanner. The behavioral experiment took place 1–2 h before the first PET scans. The procedure was based on the staircase procedure suggested by Tversky and Kahneman (1992), which is the most efficient method for estimating certainty equivalents (Paulus and Frank, 2006; Fox and Poldrack, 2009). A gamble's certainty equivalent is the amount of sure payoff at which a player is indifferent between the sure payoff and the gamble. Participants were presented with options between a gamble and a sure payoff on a computer monitor (supplemental Fig. 1, available at www.jneurosci.org as supplemental material). Gambles were presented that had an objective probability p of paying a known outcome x (and paying zero otherwise). The different combinations of p and x are shown in supplemental Table 1, available at www.jneurosci.org as supplemental material. There were 22 gambles, and half of them were 10,000 yen (~$100) gambles. Because 10,000 yen is the highest-value Japanese paper currency, 11 probabilities were used for 10,000 yen gambles to refine the estimation of weighting function. In each trial, the participants chose between a gamble and a sure payoff. The relative position (left and right) of the two options was randomized to counterbalance for order effects. The subjects were told to make hypothetical rather than actual gambles and were instructed as follows: "Two options for possible monetary gain will be presented to you. Option 1 is a sure payoff and option 2 is a gamble. For example, you will see the guaranteed 6,666 yen on one side of the monitor, and see a gamble in which you have a 50% chance of winning 10,000 yen on the other side. Make a choice between the two options according to your preference by pressing the right or left button. There is no correct answer and no time limit. Once you make a choice, the next options will be presented."

Each time a choice was made between a gamble and a sure payoff in a trial, the amount of a sure payoff in the next trial was adjusted and eight trials per each gamble were iterated to successively narrow the range including the certainty equivalents. The adjustments in the amount of a sure payoff were made in the following manner. The initial range was set between 0 and x (the gamble outcome). The range was divided into thirds. The one-third and the two-thirds intersecting points of the initial range were used as sure payoff options in trials 1 and 2. If the participant accepted the sure option of the two-thirds and rejected that of the one-third in trials 1 and 2, the middle third portion of the initial range was used as a range for trials 3 and 4. If the participant accepted both sure options of the thirds, the lower third part was then used as a range. If the participant rejected both the sure options of the thirds, the upper third part was then used. The new range was again divided into thirds and the same procedure was iterated until the participant completed trial 8. The mean of the final range was used for a certainty equivalent (supplemental Fig. 2, available at www.jneurosci.org as supplemental material). Once a certainty equivalent was estimated for a given gamble, the next gamble was chosen for estimation, and so on. The order of the gambles was randomized across the participants.

Behavioral data estimation

According to the prospect theory, the valuation V of a prospect that pays amount x with probability p is expressed as $v(x, p) = w(p)\, v(x)$, where v is the subjective value of the amount x, and w is the decision weight of the objective probability p. The utility function is usually assumed to be a power function $v(x) = x^{\sigma}$ (results are typically similar to other functions). Although several estimations of the nonlinear probability weighing function have been used in previous experiments (Lattimore et al., 1992; Tversky and Kahneman, 1992; Wu and Gonzalez, 1996), we estimated probability weighting using the one-parameter function derived axiomatically by Prelec (1998), $w(p) = \exp\{-(\ln(1/p))^{\alpha}\}$ with $0 < \alpha < 1$. This function typically fits as well as other functions with one or two parameters (Hsu et al., 2009), and because nonlinearity is fully captured by a single parameter, it is simple to correlate the degree of nonlinearity (α) across individuals with biological measures such as receptor density or fMRI signals (Hsu et al., 2009). This $w(p)$ function has an inverted-S shape with a fixed inflection point at $p = 1/e = 0.37$ (at that point the probability $1/e$ also receives decision weight $1/e$). The parameter α indicates the degree of nonlinearity. A smaller value of α (closer to 0) means a more nonlinear inflected weighting function and a higher value (closer to 1) means a more linear weighting function. At $\alpha = 1$ the function is linear. The weighting function and utility function were estimated by least-squares method.

PET scanning

PET studies were performed on ECAT EXACT HR+ (CTI-Siemens). The system provides 63 planes and a 15.5 cm field of view. To minimize head movement, a head fixation device (Fixster) was used. A transmission scan for attenuation correction was performed using a germanium 68–gallium 68 source. Acquisitions were done in three-dimensional mode with the interplane septa retracted. The first group of 18 subjects (mean age ± SD, 24.7 ± 3.8 years) was studied for both D_1 receptors and extrastriatal D_2 receptors. These 18 subjects came to the PET center twice, once each for the studies of [^{11}C]SCH23390 (*R*-(+)-7-chloro-8-hydroxy-3-methyl-1-phenyl-2,3,4,5-tetrahydro-1*H*-3-benzazepine) and [^{11}C]FLB457 ((*S*)-*N*-((1-ethyl-2-pyrrolidinyl)methyl)-5-bromo-2,3-dimethoxybenzamide). For evaluation of D_1 receptors, a bolus of 215.9 ± 9.8 MBq of [^{11}C]SCH23390 with specific radioactivities (90.1 ± 38.5 GBq/μmol) was injected intravenously from the antecubital vein with a 20 ml saline flush. The fact that [^{11}C]SCH23390 has high affinity for D_1 receptors (Ekelund et al., 2007), and that D_1 receptors are mod-

erately expressed in the extrastriatal regions (approximately one-fifth of striatal D_1 receptor density) (Ito et al., 2008) leads to good reproducibility of both striatal and extrastriatal [^{11}C]SCH23390 bindings (Hirvonen et al., 2001). Although [^{11}C]SCH23390 is a selective radioligand for D_1 receptors, it has some affinity for $5HT_{2A}$ receptors. However, $5HT_{2A}$ receptor density in the striatum is negligible compared with D_1 receptor density. $5HT_{2A}$ receptor density is never negligible in the extrastriatal regions. Although previous reports in the literature have indicated that [^{11}C]SCH23390 affinity for $5HT_{2A}$ receptors relative to D_1 receptors is negligible, a recent *in vivo* study reported that approximately one-fourth of the cortical signal of [^{11}C]SCH23390 was due to binding to $5HT_{2A}$ receptors, suggesting that cautious interpretation of the extrastriatal findings regarding this ligand is recommended (Ekelund et al., 2007). For evaluation of extrastriatal D_2 receptors, a bolus of 218.3 ± 13.9 MBq of [^{11}C]FLB457 with high specific radioactivities (238.0 ± 100.8 GBq/μmol) was injected in the same way. [^{11}C]FLB457 has very high affinity for D_2 receptors. It is a selective radioligand for D_2 receptors and has good reproducibility of extrastriatal D_2 bindings (Sudo et al., 2001). Dynamic scans were performed for 60 min for [^{11}C]SCH23390 and 90 min for [^{11}C]FLB457 immediately after the injection. Although [^{11}C]FLB457 accumulates to a high degree in the striatum, striatal data were not evaluated since the duration of the [^{11}C]FLB457 PET study was not sufficient to obtain equilibrium in the striatum (Olsson et al., 1999; Suhara et al., 1999). For radiation safety reason, striatal D_2 receptors were evaluated in the second group of the other 18 subjects [mean age ± SD, 25.7 ± SD 5.9 years]. A bolus of 218.2 ± 10.1MBq of [^{11}C]raclopride with a specific radioactivity of 451.1 ± 154.6 GBq/μmol was injected similarly. [^{11}C]Raclopride is a selective radioligand for D_2 receptors, and has good reproducibility of striatal D_2 bindings (Volkow et al., 1993). Because the density of extrastriatal D_2 receptors is less than one-tenth of striatal D_2 receptors (Ito et al., 2008), [^{11}C]raclopride is suitable for the evaluation of striatal D_2 receptors, but not of extrastriatal D_2 receptors, due to its moderate affinity for D_2 receptors. Dynamic scans were performed for 60 min. All emission scans were reconstructed with a Hanning filter cutoff frequency of 0.4 (full width at half maximum, 7.5 mm). MRI was performed on Gyroscan NT (Philips Medical Systems) (1.5 T). T1-weighted images of the brain were obtained for all subjects. Scan parameters were 1-mm-thick, three-dimensional T1 images with a transverse plane (repetition time/echo time, 19/10 ms; flip angle, 30°; scan matrix, 256 × 256 pixels; field of view, 256 × 256 mm; number of excitations, 1).

Quantification of D_1 and D_2 receptors

Because one subject felt discomfort from the head fixation device during the [^{11}C]FLB457 scan, the scan was discontinued and the data of this subject were excluded from the subsequent analysis. Quantitative analysis was performed using the three-parameter simplified reference tissue model (Lammertsma and Hume, 1996; Olsson et al., 1999). This method is well established for [^{11}C]SCH23390, [^{11}C]FLB457 and [^{11}C]raclopride (Lammertsma and Hume, 1996; Olsson et al., 1999) and is widely used (Aalto et al., 2005; Takahashi et al., 2008; McNab et al., 2009; Takahashi et al., 2010), and it allows us to quantify DA receptors without arterial blood sampling, an invasive and time-consuming procedure. The cerebellum was used as reference region because it has been shown to be almost devoid of D_1 and D2 receptors (Farde et al., 1987; Suhara et al., 1999). The model provides an estimation of the binding potential [$BP_{ND\ (nondisplaceable)}$] (Innis et al., 2007), which is defined by the following equation: $BP_{ND} = k_3/k_4 = f_2 B_{max}/\{K_d [1 + \Sigma_i F_i/K_{di}]\}$, where k_3 and k_4 describe the bidirectional exchange of tracer between the free compartment and the compartment representing specific binding, f_2 is the "free fraction" of nonspecifically bound radioligand in brain, B_{max} is the receptor density, K_d is the equilibrium dissociation constant for the radioligand, and F_i and K_{di} are the free concentration and the dissociation constant of competing ligands, respectively (Lammertsma and Hume, 1996). Based on this model, we created parametric images of BP_{ND} using the basis function method (Gunn et al., 1997) to conduct voxelwise statistical parametric mapping (SPM) analysis.

In addition to the SPM analysis, we conducted region-of-interest (ROI) analysis. The tissue concentrations of the radioactivities of [^{11}C]SCH23390, [^{11}C]FLB457 and [^{11}C]raclopride were obtained from anatomically defined ROIs. The individual MRIs were coregistered on [^{11}C]SCH23390, [^{11}C]FLB457 and [^{11}C]raclopride PET images of summated activity for 60, 90 and 60 min, respectively. The ROIs were defined on coregistered MRI with reference to the brain atlas. Given our hypothesis from the previous literature (Hsu et al., 2009), the ROIs were set on the striatum (caudate and putamen). Manual delineation of caudate and putamen ROIs was based on the dorsal caudate and dorsal putamen criteria, respectively, of Mawlawi et al. (2001). The average values of right and left ROIs were used to increase the signal-to-noise ratio for the calculations.

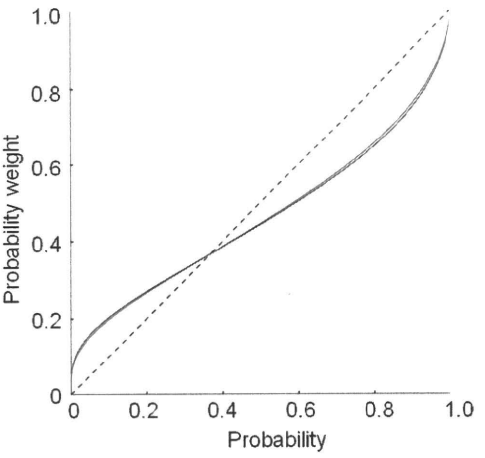

Figure 1. The fitted probability weighting function with the Prelec model. The red line represents the first group ($N = 18$ subjects) with D_1 receptors and extrastriatal D_2 receptors investigated. The black line is the second group ($N = 18$ subjects) whose striatal D_2 receptors were investigated.

Statistical analysis

SPM analysis. Parametric images of BP_{ND} of [^{11}C]SCH23390, [^{11}C]FLB457 and [^{11}C]raclopride were analyzed using the SPM2 software package (Wellcome Department of Cognitive Neurology, London, UK) running with MATLAB (MathWorks). Parametric images of BP_{ND} were normalized into MNI (Montreal Neurological Institute) template space. Normalized BP_{ND} images were smoothed with a Gaussian filter to 8 mm full-width half-maximum. Using each of the individual behavioral parameters (α and σ) as covariate, regression analyses with the BP_{ND} images and the covariates were performed. A statistical threshold of $p < 0.05$ corrected for multiple comparisons across the whole brain was used, except for a priori hypothesized regions, which were thresholded at $p < 0.001$ uncorrected ($r > 0.68$) for examination of effect size (only clusters involving 10 or more contiguous voxels are reported). These a priori ROIs included the caudate and putamen.

ROI analysis. Pearson's correlation coefficients between BP_{ND} of [^{11}C]SCH23390 and [^{11}C]raclopride in the ROIs and behavioral parameters (α and σ) were calculated using SPSS software. Because some subjects were smokers, we further calculated partial correlation coefficients between BP_{ND} of [^{11}C]SCH23390 and [^{11}C]raclopride and behavioral parameters to control for the potential influence of smoking (number of cigarettes per day).

Results

In the first group, with D_1 receptors and extrastriatal D_2 receptors investigated, the mean (SD) α of the weighting function and σ of the utility function were 0.58 (0.16) and 0.99 (0.33), respectively. The second group, in which striatal D_2 receptors were investigated, the mean (SD) α and σ were 0.56 (0.19) and 0.98 (0.18), respectively, indicating that the two groups were comparable. Averaged weighting functions and value functions of the two groups are shown in Figure 1 and supplemental Figure 3 (available at www.jneurosci.org as sup-

plemental material), respectively. Normalized parametric images of BP_{ND} of [^{11}C]SCH23390, [^{11}C]raclopride and [^{11}C]FLB457 are shown in Figure 2*A*, *B*, and *C*, respectively. The mean BP_{ND} values of [^{11}C]SCH23390 in the caudate and putamen were 1.86 ± 0.24 and 2.01 ± 0.22, and those of [^{11}C]raclopride were 3.00 ± 0.32 and 3.61 ± 0.37, respectively. Voxel-by-voxel SPM analysis revealed significant positive correlation ($r > 0.68, p < 0.001$) between striatal D_1 receptor binding and the nonlinearity parameter α of weighting function [right striatum, peak (30, −8, −4), 230 voxels; left striatum, peak (−20, −4, 8), 154 voxels] (Fig. 3*A*). Independent ROI analyses revealed that D_1 receptor binding in the putamen showed a significant correlation with α (Fig. 3*B*; Table 1), and D_1 receptor binding in the caudate showed a trend level correlation with α (Table 1). That is, people with lower striatal D_1 receptor binding tend to be more risk-seeking for low probability gambles and more risk-averse for high probability gambles. SPM analysis showed that extrastriatal D_1 binding was not correlated with α. SPM and ROI analyses revealed that neither striatal nor extrastriatal D_2 receptor binding was correlated with α. None of [^{11}C]SCH23390, [^{11}C]FLB457 and [^{11}C]raclopride binding was correlated with the power σ of the value function. Correlation analyses with controlling for the potential influence of smoking revealed identical results, indicating that the influence of smoking was minimal. The results of partial correlation analyses of ROIs between behavioral parameters (α and σ) and BP_{ND} values of [^{11}C]SCH23390 and [^{11}C]raclopride in the striatum after controlling for the potential influence of smoking are summarized in supplemental Table 2, available at www.jneurosci.org as supplemental material.

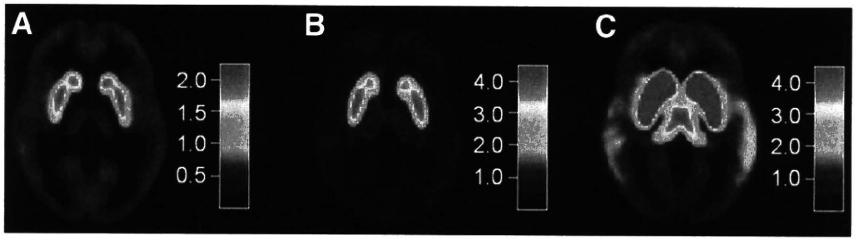

Figure 2. Maps of DA D_1 and D_2 BP, averaged across participants (axial slices at the level of $Z = 0$ of MNI coordinates). ***A***, D_1 BP, measured with [^{11}C]SCH23390 ($N = 18$ subjects). ***B***, Striatal D_2 BP, measured with [^{11}C]raclopride ($N = 18$ subjects). ***C***, Extrastriatal D_2 BP, measured with [^{11}C]FLB457 ($N = 17$ subjects). Although [^{11}C]FLB457 accumulates to a high degree in the striatum, striatal data were not evaluated because the duration of the [^{11}C]FLB457 PET study was not sufficient to obtain equilibrium in the striatum. The bar indicates the range of BP.

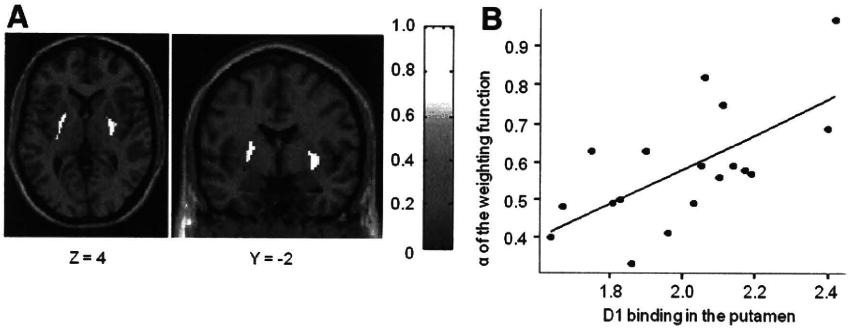

Figure 3. Correlation between nonlinearity of probabilities weighting and D_1 binding in the striatum ($N = 18$ subjects). ***A***, Image showing regions of correlation between nonlinearity parameter of weighting function and D_1 binding in the striatum. The bar shows the range of the correlation coefficient. ***B***, Plots and regression line of correlation between α (nonlinearity parameter) and binding potential of the putamen ($r = 0.66, p = 0.003$).

Table 1. Correlation between behavioral parameters (α and σ) and BP_{ND} values of [^{11}C]SCH23390 ($N = 18$ subjects) and [^{11}C]raclopride ($N = 18$ subjects) in the striatum

	α	σ
D_1 receptors		
Caudate	0.011 ($r = 0.582$)	0.717 ($r = 0.092$)
Putamen	0.003* ($r = 0.658$)	0.260 ($r = 0.280$)
D_2 receptors		
Caudate	0.305 ($r = 0.256$)	0.218 ($r = 0.305$)
Putamen	0.242 ($r = 0.291$)	0.122 ($r = 0.378$)

p values (correlation coefficients) are shown. *$p < 0.01$.

Discussion

We provided the first evidence of a relation between striatal D_1 receptor binding and nonlinear probability weighting during decision-making under risk. Based on circumstantial evidence (Kuhnen and Knutson, 2005; Wittmann et al., 2008) and a speculative review (Trepel et al., 2005), it has been suggested that curvature of the weighting function might be modulated by DA transmission. Utilizing a molecular imaging technique, we directly measured the relation between DA receptors and the nonlinearity of weighting function *in vivo*. Individuals with lower striatal D_1 receptor binding showed more nonlinear probability weighting and more pronounced overestimation of low probabilities and underestimation of high probabilities. Low D_1 receptor binding means that available receptors for phasically released DA are limited. In such case, phasic DA release in response to positive outcomes can stimulate limited D_1 receptors in the striatum. In contrast, low-level baseline tonic DA release is enough for stimulating D_2 receptors (Frank et al., 2007; Schultz, 2007). Therefore, the variability of D_2 receptor binding might have less impact on current behavioral task during which phasic DA release occurs in response to reward cue.

This molecular imaging approach allows us to broaden our understanding of the neurobiological mechanism underlying nonlinear weighting beyond the current knowledge attained by neuroeconomics fMRI. An fMRI study using a value-titration paradigm has shown that differential anterior cingulate activation during estimation of high probabilities relative to low probabilities was positively correlated with Prelec's nonlinearity parameter α across subjects (Paulus and Frank, 2006). Another fMRI study with risks of electric shocks found similar nonlinear response in the caudate/subgenual anterior cingulate (Berns et al., 2008). More recently, Hsu et al. (2009), using a simpler exposure-choice paradigm, demonstrated that Prelec's nonlinearity parameter α was negatively correlated with striatal activity during reward anticipation under risk. That is, people with a greater degree of nonlinearity in striatal activation to anticipated reward tend to overestimate low probabilities (to be risk-seeking) and underestimate high probabilities (to be risk-averse).

Exploring novelty and risk-seeking behavior are, to some extent, desirable and advantageous for the survival and develop-

ment of many species including human (Kelley et al., 2004). Being too risk-averse would lose opportunities to obtain possibly better outcomes. However, excessive risk-seeking may contribute to reckless choices such as initiation of drug use (or gambling) and transition to regular drug use (or gambling) (Kreek et al., 2005). Pathological gambling and drug addiction frequently co-occur, and it is suggested that the neurobiological mechanisms underlying the two conditions overlap (Tamminga and Nestler, 2006; Steeves et al., 2009). In fact, pharmacological therapy for drug addiction has been shown to also be effective when applied to pathological gambling (Tamminga and Nestler, 2006). Animal studies demonstrated that stimulation of D_1 receptors by a selective agonist increased risky choice and blockade of D_1 receptors decreased risky choice in rats. Although D_2 agonist/antagonist showed similar actions, their effects were not as pronounced as those of D_1 agonist/antagonist (St Onge and Floresco, 2009). A human genetic study reported that variants of the gene for D_1 receptors were linked to risky and novelty-seeking behaviors (Comings et al., 1997), although the genes for other subtypes of DA receptors are also linked to those behaviors. More recently, a PET study suggested that reduced D_1 receptor binding may be associated with an increased risk of relapse in drug addiction (Martinez et al., 2009).

The curvature of the weighting function is traditionally explained by the psychophysics of diminishing sensitivity, the idea that sensitivity to changes in probability decreases as probability moves away from the endpoints of 0 and 1 (Tversky and Kahneman, 1992). However, it has also been suggested that emotional responses to gambles influence weighting as well. In particular, the overweighting of low-probability gains may reflect hope of winning and the underweighting of high-probability gains may reflect fear of losing a "near sure thing" (Trepel et al., 2005). One study supportive of this hypothesis found more nonlinear weighting functions for gambles over emotional outcomes (kisses and shocks) than over money (Rottenstreich and Hsee, 2001). In this sense, individuals with lower striatal D_1 binding might be interpreted as showing more "emotional" decision-making.

We used a simple behavioral task with only positive outcomes to estimate weighting function in this study. Any generalization of our findings needs to be approached with caution. We make more complex decisions in the real world where both positive and negative outcomes are possible, and have to pay attention to relative differences in the magnitude of gains and losses. A computational model has suggested that tonic D_2 receptor stimulation in the striatum inhibits response to avoid negative outcomes (Frank et al., 2007), and other neurotransmitters such as serotonin and noradrenaline are thought to be involved in the complex decision-making process (Trepel et al., 2005; Frank et al., 2007; Cools et al., 2008; Doya, 2008). Using behavioral tasks with negative outcomes, future studies to investigate involvements of other neurotransmissions as well as other areas that are related to punishment or negative emotions such as the orbitofrontal cortex, insula and amygdala (Trepel et al., 2005; Pessiglione et al., 2006; Voon et al., 2010) are recommended. Furthermore, our subjects were relatively homogeneous in terms of economic status (the majority were students). Our findings might not be representative of various samples with different background and socioeconomic status. Notwithstanding this limitation, the present study illustrated that molecular imaging can provide a new research direction for neuroeconomics and decision-making studies by more directly investigating the association between striatal DA transmission and nonlinear probability weighting. This approach may shed light on neurotransmission effects on emotional and boundedly rational decision-making in our daily life. At the same time, understanding the molecular mechanism of extreme or impaired decision-making can contribute to the assessment and prevention of drug and gambling addiction and the development of novel pharmacological therapies for those addictions.

References

Aalto S, Brück A, Laine M, Någren K, Rinne J (2005) Frontal and temporal dopamine release during working memory and attention tasks in healthy humans: a positron emission tomography study using the high-affinity dopamine D2 receptor ligand [^{11}C] FLB 457. J Neurosci 25:2471–2477.

Berns GS, Capra CM, Chappelow J, Moore S, Noussair C (2008) Nonlinear neurobiological probability weighting functions for aversive outcomes. Neuroimage 39:2047–2057.

Camerer C, Loewenstein G (2004) Behavioral economics: past, present, future. In: Advances in behavioral economics (Camerer C, Loewenstein G, Rabin M, eds), pp 3–51. Princeton: Princeton UP.

Comings D, Gade R, Wu S, Chiu C, Dietz G, Muhleman D, Saucier G, Ferry L, Rosenthal RJ, Lesieur HR, Rugle LJ, MacMurray P (1997) Studies of the potential role of the dopamine D1 receptor gene in addictive behaviors. Mol Psychiatry 2:44–56.

Cools R, Roberts AC, Robbins TW (2008) Serotoninergic regulation of emotional and behavioural control processes. Trends Cogn Sci 12:31–40.

De Martino B, Kumaran D, Seymour B, Dolan RJ (2006) Frames, biases, and rational decision-making in the human brain. Science 313:684–687.

Doya K (2008) Modulators of decision making. Nat Neurosci 11:410–416.

Ekelund J, Slifstein M, Narendran R, Guillin O, Belani H, Guo NN, Hwang Y, Hwang DR, Abi-Dargham A, Laruelle M (2007) In vivo DA D1 receptor selectivity of NNC 112 and SCH 23390. Mol Imaging Biol 9:117–125.

Farde L, Halldin C, Stone-Elander S, Sedvall G (1987) PET analysis of human dopamine receptor subtypes using 11C-SCH 23390 and 11C-raclopride. Psychopharmacology (Berl) 92:278–284.

Fox C, Poldrack R (2009) Prospect theory and the brain. In: Neuroeconomics (Glimcher PW, Camerer C, Fehr E, Poldrack R, eds), pp 145–174. London: Academic.

Frank MJ, Scheres A, Sherman SJ (2007) Understanding decision-making deficits in neurological conditions: insights from models of natural action selection. Philos Trans R Soc Lond B Biol Sci 362:1641–1654.

Grace A (1991) Phasic versus tonic dopamine release and the modulation of dopamine system responsivity: a hypothesis for the etiology of schizophrenia. Neuroscience 41:1–24.

Gunn RN, Lammertsma AA, Hume SP, Cunningham VJ (1997) Parametric imaging of ligand-receptor binding in PET using a simplified reference region model. Neuroimage 6:279–287.

Hirvonen J, Någren K, Kajander J, Hietala J (2001) Measurement of cortical dopamine d1 receptor binding with 11C [SCH23390]: a test-retest analysis. J Cereb Blood Flow Metab 21:1146–1150.

Hsu M, Krajbich I, Zhao C, Camerer CF (2009) Neural response to reward anticipation under risk is nonlinear in probabilities. J Neurosci 29:2231–2237.

Innis RB, Cunningham VJ, Delforge J, Fujita M, Gjedde A, Gunn RN, Holden J, Houle S, Huang SC, Ichise M, Iida H, Ito H, Kimura Y, Koeppe RA, Knudsen GM, Knuuti J, Lammertsma AA, Laruelle M, Logan J, Maguire RP, et al (2007) Consensus nomenclature for in vivo imaging of reversibly binding radioligands. J Cereb Blood Flow Metab 27:1533–1539.

Ito H, Takahashi H, Arakawa R, Takano H, Suhara T (2008) Normal database of dopaminergic neurotransmission system in human brain measured by positron emission tomography. Neuroimage 39:555–565.

Kelley AE, Schochet T, Landry CF (2004) Risk taking and novelty seeking in adolescence: introduction to part I. Ann N Y Acad Sci 1021:27–32.

Kreek MJ, Nielsen DA, Butelman ER, LaForge KS (2005) Genetic influences on impulsivity, risk taking, stress responsivity and vulnerability to drug abuse and addiction. Nat Neurosci 8:1450–1457.

Kuhnen CM, Knutson B (2005) The neural basis of financial risk taking. Neuron 47:763–770.

Lammertsma AA, Hume SP (1996) Simplified reference tissue model for PET receptor studies. Neuroimage 4:153–158.

Lattimore P, Baker J, Witte A (1992) The influence of probability on risky choice: a parametric examination. Behav Organ 17:377–400.

Leyton M, Boileau I, Benkelfat C, Diksic M, Baker G, Dagher A (2002) Amphetamine-induced increases in extracellular dopamine, drug want-

ing, and novelty seeking: a PET/[11C] raclopride study in healthy men. Neuropsychopharmacology 27:1027–1035.

Martinez D, Slifstein M, Narendran R, Foltin RW, Broft A, Hwang DR, Perez A, Abi-Dargham A, Fischman MW, Kleber HD, Laruelle M (2009) Dopamine D1 receptors in cocaine dependence measured with PET and the choice to self-administer cocaine. Neuropsychopharmacology 34:1774–1782.

Mawlawi O, Martinez D, Slifstein M, Broft A, Chatterjee R, Hwang DR, Huang Y, Simpson N, Ngo K, Van Heertum R, Laruelle M (2001) Imaging human mesolimbic dopamine transmission with positron emission tomography: I. accuracy and precision of D2 receptor parameter measurements in ventral striatum. J Cereb Blood Flow Metab 21:1034–1057.

McNab F, Varrone A, Farde L, Jucaite A, Bystritsky P, Forssberg H, Klingberg T (2009) Changes in cortical dopamine D1 receptor binding associated with cognitive training. Science 323:800–802.

Olsson H, Halldin C, Swahn CG, Farde L (1999) Quantification of [^{11}C]FLB 457 binding to extrastriatal dopamine receptors in the human brain. J Cereb Blood Flow Metab 19:1164–1173.

Paulus MP, Frank LR (2006) Anterior cingulate activity modulates nonlinear decision weight function of uncertain prospects. Neuroimage 30:668–677.

Pessiglione M, Seymour B, Flandin G, Dolan RJ, Frith CD (2006) Dopamine-dependent prediction errors underpin reward-seeking behaviour in humans. Nature 442:1042–1045.

Prelec D (1998) The probability weighting function. Econometrica 66: 497–527.

Rangel A, Camerer C, Montague PR (2008) A framework for studying the neurobiology of value-based decision making. Nat Rev Neurosci 9:545–556.

Rottenstreich Y, Hsee CK (2001) Money, kisses, and electric shocks: on the affective psychology of risk. Psychol Sci 12:185–190.

Schultz W (2007) Behavioral dopamine signals. Trends Neurosci 30:203–210.

Steeves TD, Miyasaki J, Zurowski M, Lang AE, Pellecchia G, Van Eimeren T, Rusjan P, Houle S, Strafella AP (2009) Increased striatal dopamine release in Parkinsonian patients with pathological gambling: a [^{11}C] raclopride PET study. Brain 132:1376–1385.

St Onge JR, Floresco SB (2009) Dopaminergic modulation of risk-based decision making. Neuropsychopharmacology 34:681–697.

Sudo Y, Suhara T, Inoue M, Ito H, Suzuki K, Saijo T, Halldin C, Farde L (2001) Reproducibility of [^{11}C]FLB 457 binding in extrastriatal regions. Nucl Med Commun 22:1215–1221.

Suhara T, Sudo Y, Okauchi T, Maeda J, Kawabe K, Suzuki K, Okubo Y, Nakashima Y, Ito H, Tanada S, Halldin C, Farde L (1999) Extrastriatal dopamine D2 receptor density and affinity in the human brain measured by 3D PET. Int J Neuropsychopharmcol 2:73–82.

Takahashi H, Kato M, Takano H, Arakawa R, Okumura M, Otsuka T, Kodaka F, Hayashi M, Okubo Y, Ito H Suhara T (2008) Differential contributions of prefrontal and hippocampal dopamine D1 and D2 receptors in human cognitive functions. J Neurosci 28:12032–12038.

Takahashi H, Takano H, Kodaka F, Arakawa R, Yamada M, Otsuka T, Hirano Y, Kikyo H, Okubo Y, Kato M, Obata T, Ito H, Suhara T (2010) Contribution of dopamine D1 and D2 receptors to amygdala activity in human. J Neurosci 30:3043–3047.

Tamminga CA, Nestler EJ (2006) Pathological gambling: focusing on the addiction, not the activity. Am J Psychiatry 163:180–181.

Tom SM, Fox CR, Trepel C, Poldrack RA (2007) The neural basis of loss aversion in decision-making under risk. Science 315:515–518.

Trepel C, Fox CR, Poldrack RA (2005) Prospect theory on the brain? Toward a cognitive neuroscience of decision under risk. Brain Res Cogn Brain Res 23:34–50.

Tversky A, Kahneman D (1992) Advances in prospect theory: cumulative representation of uncertainty. J Risk Uncertain 5:297–323.

Volkow ND, Fowler JS, Wang GJ, Dewey SL, Schlyer D, MacGregor R, Logan J, Alexoff D, Shea C, Hitzemann R, Angrist B, Wolf AP (1993) Reproducibility of repeated measures of carbon-11-raclopride binding in the human brain. J Nucl Med 34:609–613.

von Neumann J, Morgenstern O (1944) Theory of games and economic behavior. Princeton: Princeton UP.

Voon V, Pessiglione M, Brezing C, Gallea C, Fernandez HH, Dolan RJ, Hallett M (2010) Mechanisms underlying dopamine-mediated reward bias in compulsive behaviors. Neuron 65:135–142.

Wittmann BC, Daw ND, Seymour B, Dolan RJ (2008) Striatal activity underlies novelty-based choice in humans. Neuron 58:967–973.

Wu G, Gonzalez R (1996) Curvature of the probability weighting function. Manage Sci 42:1676–1690.

Zack M, Poulos CX (2004) Amphetamine primes motivation to gamble and gambling-related semantic networks in problem gamblers. Neuropsychopharmacology 29:195–207.

Psychiatry and Clinical Neurosciences 2011; 65: 191–198 doi:10.1111/j.1440-1819.2011.02189.x

Regular Article

Functional magnetic resonance imaging study on the effects of acute single administration of paroxetine on motivation-related brain activity

Toshiyuki Marutani, MD,[1,2] Noriaki Yahata, PhD,[3,4] Yumiko Ikeda, MS,[3] Takehito Ito, PhD,[1] Manami Yamamoto, PhD,[1] Masato Matsuura, MD, PhD,[5] Eisuke Matsushima, MD, PhD,[2] Yoshiro Okubo, MD, PhD,[6] Hidenori Suzuki, MD, PhD[3] and Tetsuya Matsuda, PhD[1]*

[1]*Tamagawa University Brain Science Institute,* [2]*Section of Liaison Psychiatry & Palliative Medicine, Graduate School of Tokyo Medical & Dental University,* [3]*Department of Pharmacology, Nippon Medical School,* [4]*Department of Neuropsychiatry, Graduate School of Medicine, University of Tokyo,* [5]*Section of Biofunctional Informatics, Graduate School of Allied Health Sciences, Tokyo Medical and Dental University, and* [6]*Department of Neuropsychiatry, Nippon Medical School, Tokyo, Japan*

Aim: The aim of the present study was to investigate the effects of acute paroxetine administration on brain activity related to motivation.

Methods: Sixteen healthy subjects participated in a randomized, single-blind, no-drug/placebo-controlled, cross-over study. After administration of no drug, placebo or paroxetine (selective serotonin reuptake inhibitor; 20 mg), subjects underwent functional magnetic resonance imaging while performing a monetary incentive delay task. We analyzed the differences in brain activities of the reward anticipation/motor preparation period that are subject to motivational modulation. For this purpose, we subdivided the incentive trials on the basis of whether the reaction times (RT) were slower or faster than the subject's mean RT (slow RT and fast RT trials).

Results: No drug and placebo showed robust activation differences in the globus pallidus and putamen for the fast RT trials compared to the slow RT trials, whereas paroxetine showed none. Paroxetine showed significantly lower activations in the globus pallidus, insula, putamen and dorsolateral prefrontal cortex compared to no drug in the fast RT trials.

Conclusions: Paroxetine single acute administration diminished brain activity induced by motivation in healthy subjects. This may partially explain the increased lack of motivation seen in patients with relatively mild symptoms after taking a dose of paroxetine for the first time.

Key words: functional magnetic resonance imaging, motivation, paroxetine, reaction time, reward anticipation.

SELECTIVE SEROTONIN REUPTAKE inhibitors (SSRI) are first-line drugs for the treatment of major depressive disorder (MDD). MDD is characterized by disturbances in emotion, motivation and behavior in the presence of autonomic nervous symptoms.[1] A core symptom of MDD includes decreased motivation,[2,3] which SSRI sometimes rather aggravate in some patients.[4–6]

Motivational processing includes reward anticipation, motor preparation and related processes, including arousal and attention.[7,8] Several pharmacological functional magnetic resonance imaging (fMRI) studies have assessed the functions and/or mechanisms of SSRI related to motor, attention and reward. The effects of SSRI on motor function,[9,10] attention,[11] loss/no-loss comparison[12] and neural

Correspondence: Tetsuya Matsuda, PhD, Tamagawa University Brain Science Institute, 6-1-1, Tamagawa Gakuen, Machida, Tokyo 194-8610, Japan. Email: tetsuya@lab.tamagawa.ac.jp
Received 15 September 2010; revised 23 December 2010; accepted 23 December 2010.

processing of both rewarding and aversive stimuli[13] in healthy subjects have been studied by fMRI. McCabe reported that seven days of citalopram treatment diminished the brain activity induced by deliveries of rewards and aversive stimuli. They used primary rewards, chocolate taste and unpleasant strawberry taste as stimuli. Their conclusion indicated that the results could explain the experience of emotional blunting described by some patients during SSRI treatment.[13–15]

Decrease in motivation is also clinically observed after taking an initial dosing.[16] We have clinically observed some patients, especially patients with mild symptoms who reported decreased motivation after taking an initial dose of SSRI. Then, in the present study, we focused on the effects of an SSRI single acute administration on brain activity during motor preparation and reward anticipation, which are subject to motivational modulation. For this purpose, we used a monetary incentive delay (MID) task.[17] This task has been used in numerous reward-processing studies, and variations of the MID task have been used in a variety of other research.[18–20] Regardless of the details, the reward anticipation/motor preparation period and the subsequent button press during the task are essential. It is likely that the subject's motivations fluctuate over repeated trials of the MID task, and this is reflected in reaction time (RT). We expected that paroxetine would attenuate brain activity induced by motivation.

METHODS

Subjects

Sixteen healthy subjects participated in this study, but two were excluded because of an extremely low hit rate (less than 60%). Fourteen healthy subjects (eight men, mean age ± SD: 31 ± 3.8 years) were included in the final analysis. All subjects were native Japanese speakers and right-handed, as assessed by the Edinburgh Handedness Inventory. They filled out a questionnaire about their medical history and medications and were then interviewed by a medical staff member. They had no history of present or past psychiatric illnesses, neurological disorders, significant physical illnesses or head injuries, and no alcohol- or drug-related problems. They had not taken any types of medication for at least 1 day prior to scanning.

After a complete explanation of the study, including the possible side-effects of paroxetine, written informed consent was obtained from all the subjects and all the subject identifiers were removed. The protocol was approved by the local ethics committee.

Drug administration

We chose paroxetine as the SSRI for this study because it has the highest affinity for the human serotonin (5-HT) transporter among SSRI and other antidepressants according to radioligand binding assay studies[21–23] with a reported equilibrium dissociation constant (K_D) of 0.13 ± 0.01 nmol.

All subjects were examined after administration of paroxetine (S, 20 mg [minimally effective dose] paroxetine hydrochloride hydrate tablet), placebo (P, 12 mg lactobacillus bifidus tablet) or no drug (N) in a randomized, single-blind, no drug/placebo controlled, cross-over design. Three to 43 days (average 14.0 ± 13.7 days) passed between experiments. The order of drug administration was counterbalanced across subjects. The drug administration order consisted of six combinations (N-P-S, N-S-P, P-N-S, P-S-N, S-N-P, S-P-N) and we randomly assigned each combination to each subject.

The maximum drug concentration time (Tmax) of paroxetine 20 mg was reported to be 5.05 ± 1.22 h in healthy Japanese subjects.[24] Accordingly, placebo (P) and paroxetine (S) were given 5–5.5 h before initiating scanning to ensure maximum and stable plasma concentrations.

A previous positron emission tomography study suggests that 80% 5-HT transporter blockade is important for therapeutic effect of SSRI.[25] A single dosing of minimum therapeutic dose of an SSRI showed around 80% 5-HT transporter occupancy, which was almost the same as long-term dosing data.[26] Accordingly, a single dosing of paroxetine 20 mg of this study should have enough 5-HT transporter occupancy for therapeutic effect.

Reward task

Subjects performed an incentive task during functional scanning after a short pre-scanning training task. The task paradigm was an event-related design. The task was created with E-Prime 1.2 (Psychology Software Tools), which consisted of 98 7–8-s trials with 4-s inter-trial intervals (approx. 19 min. total). During each trial, subjects were shown one of three cue shapes (500 ms), a fixed crosshair during a variable delay (2500–3500 ms), and they responded with

a button press during the presentation of a gray square target (500 ms). They were then shown a fixed yellow crosshair (3000 ms) and this was followed by feedback (500 ms) notifying subjects if they had gained the points indicated by the cue, gained no points (= 0 point), or failed to press the button within 500 ms. The inter-trial interval was set to 4000 ms.

The cues signaled the possibility of no gain, 0 points ($n = 10$; denoted by a circle), 100 points ($n = 44$; denoted by a circle with one horizontal line) or 500 points ($n = 44$; denoted by a circle with three horizontal lines). There were three pseudorandom and predetermined orders of trials presented to subjects depending on experimental order, i.e. the combinations of medication and trial presentation order were counterbalanced.

Before scanning, subjects were instructed that the duration of target presentation was fixed to 500 ms but the button press limits differed from trial to trial. Fourteen 100-point cue and 500-point cue trials were predetermined to have a feedback of 0 points despite any efforts. In eight of these 28 trials, RT were not collected and were excluded from the analysis. The other trials required a fixed 500-ms time limit for the button press. If the subject did not respond in the appropriate interval, the message 'Press the button!' was displayed. We asked subjects to respond as quickly as possible to gain the maximum number of points, but the points earned were not reflected in the payment for participation in the study. Subjects were also asked to respond within the target presentation time even if the cue was a circle without line (potential 0 points). The total points earned were displayed at the end of the session.

During the original MID task,[17] RT were collected during the practice session so that the task difficulty level was set to achieve a success rate of 66%. However, we fixed the target duration to 500 ms so that the hit rate would reflect subjects' efforts more accurately. We also performed more trials to compare the effects of differences of RT in incentive trials. To maintain cue incentives, predetermined trials of gain cued with non-gain feedback were intermixed. Subjects were not told of their running point totals to minimize possible confounding effects.

fMRI data acquisition

The fMRI scans were acquired with a 3T Siemens MAGNETOM Trio Tim system scanner (Siemens, Erlangen, Germany). A total of 575 functional images were taken with a T2*-weighted gradient echo planer imaging sequence (TE = 25 ms; TR = 2000 ms; FA = 90°; matrix 64 × 64; FOV 192 × 192 cm) sensitive to the blood oxygenation level dependent (BOLD) contrast. Whole brain coverage was obtained with 34 axial slices (thickness 4 mm; in-plane resolution 3 × 3 mm).

Behavioral data analysis

For each drug condition for each subject, the mean RT to the target was calculated. Trials in which subjects did not press the button within the time limit were excluded from this calculation. Since the goal of this study was to investigate motivational motor preparation, we divided the RT of the incentive trials (100 and 500 points) on the basis of whether the RT were slower or faster than the subject's mean RT (RTslow and RTfast). For the purpose of this analysis, the 100- and 500-point trials were pooled to increase the sample set; there were no significant differences in hit rate or proportion of successful button presses among drug conditions for the different point trials. The mean RT of the slow RT and the fast RT trials were calculated, and these data were entered into a 3 (drug: non-drug, placebo, and paroxetine) × 2 (RT: slow and fast)-repeated-measures ANOVA using SPSS 16.0 J (SPSS Japan, Tokyo, Japan). The level of significance was set at 0.05.

fMRI data analysis

Image pre-processing and data analysis were performed with the statistical parametric mapping software package, SPM5 (Wellcome Department of Imaging Neuroscience, London, UK) running MATLAB 2007a (Mathworks, Natick, MA, USA). During pre-processing, the echo planer images were corrected for sequential slice timing, and all images were realigned to the first image to adjust for possible head movements. The realigned images were then spatially normalized to a standard Montreal Neurological Institute (MNI) template.[27] After normalization, all scans had a resolution of $2 \times 2 \times 2$ mm^3. Functional images were spatially smoothed with a 3-D isotropic Gaussian kernel (full width at half maximum of 8 mm). Low-frequency noise was removed by applying a high-pass filter (cut-off period = 192 s) and the default correction for AR1 auto correlation was performed for the fMRI time series at each voxel. A temporal smoothing function

was applied to the fMRI time series to enhance the temporal signal-to-noise ratio. Significant hemodynamic changes for each condition were examined using the general linear model with boxcar functions convoluted with a hemodynamic response function. Statistical parametric maps for each contrast of t-statistic were calculated on a voxel-by-voxel basis.

We then assessed the RT effect for each drug condition and the drug effect for the slow or fast RT during reward anticipation. We divided the trials into slow and fast RT trials, and we created the t-contrasts for the anticipation period between the offset of cue presentation and the onset of target presentation for the three different drug conditions in single-subject analysis (Nslow, Nfast, Pslow, Pfast, Sslow, Sfast).

A random effects analysis was performed to examine for population-wide effects. First, we used a 3 (medication: no drug, placebo and paroxetine) × 2 (RT: fast and slow) full factorial design to investigate brain activation between the different RT trials under each drug condition. There were significant activations for Nfast > Nslow in basal ganglia and primary motor cortex of which evident correlations have been revealed with reward anticipation[17,18,28,29] and motor preparation,[30] whereas activations for Pfast > Pslow and Sfast > Sslow were almost none. Then, to focus on regional activations in the reward anticipation and motor preparation-related areas in placebo and paroxetine, after paired *t*-tests were applied to Nfast > Nslow at the $P < 0.001$ level, uncorrected, with a voxel threshold of k = 10, we proceeded to a region-of-interest (ROI) analysis.

RESULTS

Behavioral data

The average hit rate of 90 trials was 92.9 ± 5.5%, 95.5 ± 4.2%, and 92.8 ± 6.7% for no drug, placebo, and paroxetine, respectively.

The average RT of all the trials and of the incentive (100 and 500 points) trials were 297.42 ± 38.69 ms and 294.02 ± 42.66 ms, 294.03 ± 40.31 ms and 290.45 ± 46.69 ms, 299.77 ± 38.96 ms and 298.08 ± 44.72 ms, under no drug, placebo and paroxetine conditions, respectively. There were no significant differences among three drug conditions.

Then we subdivided the RT of each incentive trial based on their relationship to the subject's mean RT, and the mean RT of each group, RTslow and RTfast, were compared for each drug treatment group.

A 3 (drug: non-drug, placebo, and paroxetine) × 2 (RT: slow and fast)-repeated-measures ANOVA revealed an effect of RT, $F_{1,13} = 398.73$, $P < 0.001$. Post hoc analyses with Bonferroni correction showed significant differences between RTslow and RTfast for each drug condition. RTslow and RTfast were 329.70 ± 27.04 ms and 258.34 ± 19.12 ms, 327.64 ± 31.61 ms and 253.25 ± 24.36 ms, 334.74 ± 30.04 ms and 261.43 ± 20.26 ms under no drug, placebo and paroxetine conditions, respectively. However, no significant differences were detected in the same RT (slow or fast) group among the different drug conditions.

fMRI data

The significantly activated areas for Nfast > Nslow were left primary motor cortex (T = 8.50), left globus pallidus (GP) (T = 5.95), right GP (T = 5.14), left dorsolateral prefrontal cortex (DLPFC) (T = 5.57), left transverse temporal gyrus (T = 5.26), right transverse temporal gyrus (T = 5.26), left thalamus (T = 4.87), right thalamus (T = 3.53), left insula (T = 4.71), right insula (T = 4.69), left putamen (T = 4.41), right putamen (T = 4.57), vermis (T = 4.50), right nucleus accumbens (NAcc) (T = 4.49) and left caudate (T = 4.27).

To investigate motivation-related areas under placebo and paroxetine conditions, we then performed a ROI analysis for the peak voxel of the regions significantly activated in Nfast > Nslow whole brain *t*-test. The ROI were selected based on previous fMRI studies of reward anticipation; GP,[28] insula,[27,29] putamen,[17,18,29] NAcc,[17] caudate,[29] DLPFC[31] and motor preparation; primary motor cortex.[30] The MNI coordinates [x y z] of ROI were left GP [−24 −10 0], right GP [20 −10 0], left insula [−38 −14 10], right insula [40 2 8], left putamen [−22 8 −2], right putamen [28 4 8], right NAcc [10 10 −14], left caudate [−6 12 4], left DLPFC [−36 32 26] and left primary motor cortex [−32 −22 54]. We collected beta values of each ROI and entered the data into 3 (drug conditions: N, P, S) × 2 (RT: slow, fast)-repeated-measures ANOVA using SPSS 16.0J. The level of significance was set at 0.05.

This ROI analysis using an ANOVA with repeated measures revealed a significant interaction between drug and RT in left insula ($F_{2,26} = 4.406$, $P = 0.022$), right insula ($F_{2,26} = 5.379$, $P = 0.011$), right NAcc ($F_{2,26} = 3.387$, $P = 0.049$), left primary motor cortex ($F_{2,26} = 4.016$, $P = 0.030$), a significant drug effect in

right insula ($F_{1,13} = 6.948$, $P = 0.021$) and left primary motor cortex ($F_{2,26} = 7.894$, $P = 0.002$), a significant RT effect in left GP ($F_{1,13} = 1.573$, $P < 0.0001$), right GP ($F_{1,13} = 37.957$, $P < 0.0001$), right insula ($F_{1,13} = 6.948$, $P = 0.021$), left putamen ($F_{1,13} = 45.757$, $P < 0.0001$), right putamen ($F_{1,13} = 13.968$, $P = 0.002$), right NAcc ($F_{1,13} = 5.755$ $P = 0.032$), left caudate ($F_{1,13} = 10.553$, $P = 0.006$), left DLPFC ($F_{1,13} = 10.568$, $P = 0.006$) and left primary motor cortex ($F_{1,13} = 38.179$, $P < 0.0001$).

Post hoc analysis with Bonferroni correction showed there were significant differences between paroxetine and placebo in only the left primary motor cortex, Pslow and Sslow ($P = 0.003$), Pfast and Sfast ($P = 0.008$), in which the activations were greater under placebo treatment (Fig. 1j). In the absence of drug or placebo treatment, the fast RT trials (Nfast) showed significantly higher activation than the fast RT trials of paroxetine condition (Sfast) in left GP ($P = 0.023$), left insula ($P = 0.008$), right insula ($P = 0.007$), right putamen ($P = 0.008$), left DLPFC ($P = 0.022$) and left primary motor cortex ($P = 0.003$) (Fig. 1a,c,d,f,i,j), which was not shown in comparison between the slow RT trials. There were no significant differences between placebo and no drug in any of the ROI.

Considering the way the ROI were defined, it was natural that there were significant differences between Nslow and Nfast in all the ROI. In paroxetine conditions, Sfast was significantly more activated than Sslow in only the left primary motor cortex (Fig. 1j). When subjects were given placebo, Pfast activation was greater than Pslow only in the left GP ($P = 0.045$), left putamen ($P = 0.007$) and left primary motor cortex ($P = 0.042$) (Fig. 1a,e,j).

DISCUSSION

Disturbances in motivation and motor activity are seen in MDD and these symptoms are sometimes exacerbated by SSRI in some patients. To investigate this paradoxical effect, we wish to use fMRI to monitor affected patients in response to drug therapy. However, as a first step, we studied normal subjects following a single dose of the SSRI paroxetine.

In this collection of normal subjects, there were no differences among the three drug conditions within each of the average RT of the whole, no incentive, incentive and subdivided RT trials. Thus, paroxetine administration did not affect subject behavior or performance globally. The average RT of no incentive and incentive trials showed no significance, which might be induced by the instruction for the subjects to press the button within the short duration of 500 ms even when the cue was no incentive.

Then, we investigated brain activations between the slow RT and the fast RT trials, which were behaviorally subdivided with significance, within treatment groups. The fast RT trials recruited greater activation in the GP, insula, putamen, NAcc, DLPFC, caudate and primary motor cortex than slow RT trials under no drug treatment. Under placebo conditions, the fast RT trials recruited greater activation in the GP, putamen and primary motor cortex. However, the paroxetine condition showed greater activations in the fast RT trials compared to the slow RT trials only in the primary motor cortex. These results indicated paroxetine desensitized RT influence on reward-anticipation-related brain activity, meanwhile no drug and placebo conditions reflected RT influence fully or partially in the reward-related areas.

In the next step, we looked into the activation differences in the same RT (slow or fast) group among the different drug conditions. Paroxetine significantly suppressed activation in the left GP, bilateral insula, right putamen and left DLPFC as reward-anticipation-related areas compared to no drug in the fast RT trials reflecting higher motivation, not in the slow RT trials reflecting lower motivation.

In the primary motor cortex, the activation under paroxetine administration was significantly weaker than no drug in the fast RT trials only, but weaker than placebo in both fast and slow RT trials. Besides, the fast RT trials were activated greater than the slow RT trials in all three drug conditions. Thus, the characteristics shown in the reward-related areas collapsed in the primary motor cortex, although paroxetine reduced activation compared to no drug and placebo in any case.

Taken together, paroxetine attenuated the brain activity in the reward-anticipation-related areas between the subdivided RT groups and compared to no drug in the more motivated fast RT trials. When anhedonia, one of the major symptoms of MDD, is considered as decreased motivation and sensitivity to rewarding experiences, our results suggest that a single dose of paroxetine may create a relatively anhedonic state in healthy subjects.